Renewable and Sustainable Energy Reviews 97 (2018) 233–258

Contents lists available at ScienceDirect

Renewable and Sustainable Energy Reviews

journal homepage: www.elsevier.com/locate/rser

Model development for the growth of microalgae: A review

Pooya Darvehei[a], Parisa A. Bahri[a,*], Navid R. Moheimani[b]

[a] School of Engineering and Information Technology, Murdoch University, Murdoch 6150, Western Australia, Australia
[b] Algae R & D Centre, Scool of Veterinary and Life Sciences, Murdoch University, Murdoch 6150, Western Australia, Australia

ARTICLE INFO

Keywords:
Modelling
Microalgae
Outdoor cultivation
Growth

ABSTRACT

Despite attracting many attentions in the past decades, microalgal cultivation still faces many challenges for industrialisation. Growth, as one of the most crucial characteristics of a microalgal cultivation system, has been a significant subject for modelling. This paper presents a review of available models in the literature regarding the effect of process parameters such as light, temperature, nutrients, oxygen accumulation, salinity, and pH and carbon, on the growth rate of microalgal cells to understand their application in large-scale microalgal production. The existing models are classified based on the process conditions or parameters they considered in the formulation, and where multiple parameters were included the model was broken into separate functions, and each function was presented in the associated section. The most prominent result of this review is the huge gap between models and their validity for outdoor systems. It seems that to find suitable models for a real condition application, a new pathway is needed where models are developed based on the behaviour of the outdoor cultures in long-term. There are some effects such as adaptation which are difficult to model in short-term modelling while if the long-term approach is used these effects can be considered negligible. These characteristics of outdoor cultivation help in simplification of the models and less struggle in their validation. Moreover, using saline water is an effective way to improve the viability of algal production which requires understanding the relationship between growth and salinity of the medium. Such models are missing in the literature.

1. Introduction

Microalgae are unicellular photosynthetic organisms with multiple beneficial characteristics that can potentially be used to overcome some of today's issues. They have high carbon dioxide fixation rate which can be used in flue gas treatment and the emission rate of this gas [1–3]. They use nutrients such as phosphorus and nitrogen which can be provided from industrial or municipal wastewater, making them a suitable option for waste water treatment [4–6]. Moreover, in case of marine microalgae there is no need for potable water since they can grow in saline water which facilitates the provision of water for large scale cultivation [7]. Another key attribute of microalgae is their low land requirement. They use significantly less area to grow compared to other crops due to their high photosynthetic efficiency per area [8–10]. Microalgae can be cultivated even in non-arable lands; thus, they do not impact agricultural land availability [2,8,11]. In addition to these traits, microalgae are capable of producing multiple valuable products which can be used in various industries such as food, cosmetics, pharmaceutical, etc [3,12–14]. One of the products that have attracted many attentions is biofuel. Algal biofuel is produced from the lipid stored in algal cells [15] which is extracted and converted to biodiesel. High productivity, being renewable, carbon emission mitigation, compatibility of algal biofuel with current diesel engines, and its low pollution are just a few of many advantages of using microalgae as a source of biofuel [3,16–18]. However, production of algal biofuel is still in the research stage and has not been fully commercialised yet [19].

Various systems are common for the algal cultivation of which closed photobioreactors (PBR), and open ponds are used more frequently. While construction and operation of open ponds are easy and relatively inexpensive, they have some disadvantages such as poor illumination and loss of water due to evaporation [20]. Also compared to closed PBRs, open ponds have the high risk of contamination which can directly affect production costs and annual productivity [21].

On the pathway to mass production, many process issues need to be resolved, and the growth and biomass production of algae should be well understood and optimised to make efficient operation and process control viable [22]. An important step for this purpose is mathematical modelling in which the effect of each process condition (temperature, light, etc.) is mathematically related to the key production parameters (growth rate, productivity, etc.) so that the effect of every change in the process conditions can be observed without the necessity to experimentally test the effects separately. Modelling kinetic of algal growth is

* Corresponding author.
E-mail addresses: p.darvehei@murdoch.edu.au (P. Darvehei), P.Bahri@murdoch.edu.au (P.A. Bahri).

https://doi.org/10.1016/j.rser.2018.08.027
Received 21 March 2018; Received in revised form 27 July 2018; Accepted 20 August 2018
Available online 04 September 2018
1364-0321/

vital for both estimation and optimisation of production parameters and control of process conditions which is of great importance in the industrialisation of algal biofuel production. For a model to be reliable, all the influential process conditions should be included in it which is difficult but crucial to do. Many process conditions influence the growth of microalgae and to control and optimise the industrial production of algal biofuel, an accurate mathematical model is vital. A successful model should include the effects of all parameters and their contribution, and when it is joint with reactor model should be able to predict the performance and productivity of a cultivation system for different operating conditions.

This paper presents a review of the existing models and how their formulations evolved over time to become more accurate. Although all the current models are listed in the tables to show this evolvement; only the most prominent models have been discussed and compared. Finally, the effectiveness of current models for large-scale production is discussed to elaborate a pathway to improve modelling approaches and make the models more applicable in real conditions. While many of these models have been reviewed to see their performance in laboratory scale, the novelty of this study is in two folds: (1) understanding how the current models can be adapted for use in large-scale production of microalgae, and (2) realising the gap in research regarding modelling the simultaneous impact of various factors such as salinity, light, and temperature.

2. Effective process conditions

In the past century, many studies were conducted to understand the impact of each process parameter on the growth and productivity of algal cultures. The parameters that are discussed in this review are light, temperature, nutrients, pH, salinity, and dissolved oxygen. The effects of these parameters have been studied through many experiments and many models have been suggested, of which a summary of prominent ones can be found here.

2.1. Light

Algae use light as a source of energy for photosynthesis, and therefore it is the most important parameter in the modelling of microalgal growth. Microalgal cells experience three light zones based on the intensity of the light (See Fig. 2): (1) photolimeted, (2) photosaturated, and (3) photoinhibited zone. A common phenomenon inside a turbid media like algae culture is light attenuation, where light intensity decreases as it goes deeper into the media [23] due to absorption of light by cells, and as the photons penetrate into the culture, more of them are absorbed [24]. To show this effect, usually Beer-Lambert Law is used which suggests that light intensity exponentially decreases with depth [25–27].

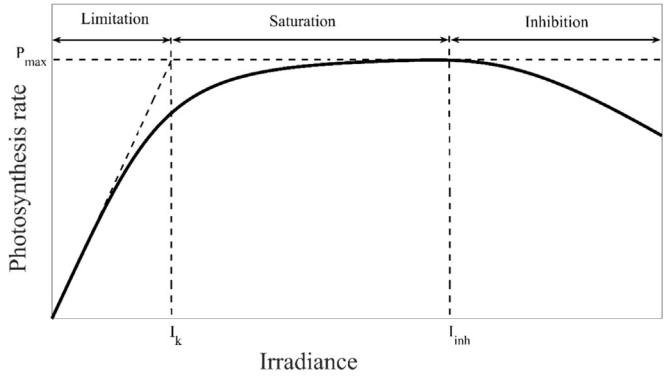

Fig. 1. A schematic of PI curve showing three light regions: (1) light limited, (2) light saturated, and (3) light inhibited.

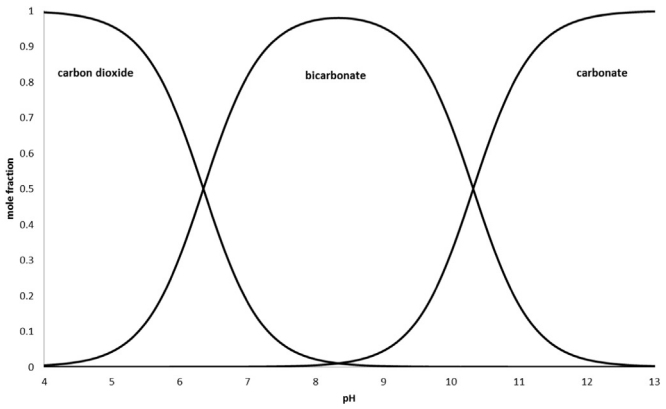

Fig. 2. Distribution of inorganic carbon forms with pH.

$$I = I_0 e^{-kz} \quad (1)$$

Where I is light intensity, I_0 is light intensity entering the media perpendicular to surface, z is depth, and k is attenuation rate. Although this relation is used widely, researchers have used different definitions for k and how it is calculated. Some researchers described it as a linear function of biomass concentration [28] or chlorophyll concentration [29], while others related k to both chlorophyll as well as biomass concentration in the media and even took into account a constant which describes the behaviour of the culture without any cells [25]. Sukenik et al. [30] assumed light attenuation rate to be a linear function of just chlorophyll amount while this dependency varies for different wavelengths. Despite its popularity, Beer-Lambert Law is based on the assumption that light is not scattered in the media which is not correct when it comes to microalgal cultures. Therefore, some researchers proposed models taking into account light scattering in order to overcome this issue [31,32].

Another factor that plays a vital role in the light exposure of algae is hydrodynamics of the culture, and how cells move within the media as when they are closer to the light source, they will be subject to more light and vice versa. This effect is critically important to determine how much light a cell may absorb and from which photosynthesis and growth rate can be calculated. Most attempts in modelling the effect of light focused on equations to describe photosynthesis and light relationship (commonly presented in form of PI curve) [33]. Photosynthesis in this relationship is expressed in various forms such as electron transfer rate (ETR), oxygen evolution, and carbon dioxide consumption, and sometimes is replaced by specific growth rate. Despite the differences between these forms, all result in the same shape of PI curve [22,34,35].

Many models have been suggested in the last few decades, a summary of which can be seen in Table 1, but here we are reviewing the details of the most prominent models. One of the earliest models that can be found in the literature was suggested by Baly [36] and later used by Tamiya [37], reporting that based on their experiments this function had approximately the same shape as their results. This equation is similar to the renowned equation proposed by Monod [38] for effect of substrates on growth of bacteria which is widely used for microalgal growth as well. In this equation, if substrate concentration is replaced by irradiance, it results in Baly and Tamiya's equation. This equation contains two key elements: 1) the maximum specific growth rate (μ_{max}) which indicates the maximum achievable specific growth rate when culture is in light saturated condition, 2) light half-saturation constant (K_I) at which the specific growth rate is half its maximum value. Parameter K_I is often compared to light saturation irradiance (I_k), which is the irradiance that defines light saturated region (Fig. 1). In this model the difference between two parameters are significant as K_I is associated with half the amount of maximum specific growth rate while at I_k the μ almost reaches its maximum value. This difference is

Table 1
Models describing the effect of light.

Source	Formula		System	Alga	Parameters
Tamiya et al. [37] **a.k.a. Monod model**	$\mu = \mu_{max}\frac{I}{I+K_I}$	(1)	Indoor	Chlorella ellipsoidea	
Lee et al. [33]			Indoor	*Spirulina platensis*	$\mu_{max} = 0.1351(h^{-1})$ $K_I = 13.9136(W/m^2)$
Molina Grima et al. [59]			Indoor	*Isochrysis galbana*	*at* $820\mu Em^{-2}s^{-1}$ $\mu_{max} = 0.109h^{-1}$ $K_I = 763.7\mu Em^{-2}s^{-1}$ *at* $1630\mu Em^{-2}s^{-1}$ $\mu_{max} = 0.0514h^{-1}$ $K_I = 177.2\mu Em^{-2}s^{-1}$ *at* $3270\mu Em^{-2}s^{-1}$ $\mu_{max} = 0.0448h^{-1}$ $K_I = 769.2\mu Em^{-2}s^{-1}$
Jeon et al. [69]			Indoor	*Haematococcus pluvialis*	*cell concentration* $0.215gL^{-1}$ $P_{max} = 43.5mgg^{-1}h^{-1}$ $K_I = 177.2\mu Em^{-2}s^{-1}$ *cell concentration* $0.123gL^{-1}$ $P_{max} = 51.7mgg^{-1}h^{-1}$ $K_I = 254.4\mu Em^{-2}s^{-1}$
Haario et al. [70]			Outdoor	Diatom	$\mu_{max} = 0.0886day^{-1}$ $K_I = 61.9(W/m^2)$
				Chrysophycea	$\mu_{max} = 0.0465day^{-1}$ $K_I = 115(W/m^2)$
				Cyanobacteria	$\mu_{max} = 0.329day^{-1}$ $K_I = 16.4(W/m^2)$
				Minor species	$\mu_{max} = 0.212day^{-1}$ $K_I = 134(W/m^2)$
Filali et al. [71]			Indoor	*Chlorella vulgaris*	$\mu_{max} = 0.08h^{-1}$ $K_I = 0.14\mu Es^{-1}10^9cell^{-1}$
Franz et al. [72]			Indoor	*Chlamydomonas reinhardtii*	$\mu_{max} = 1.4day^{-1}$ $K_I = 215\mu mol.m^{-2}.\ s^{-1}$
Ifrim et al. [73]			Indoor	*Chlamydomonas reinhardtii*	$K_I = 120\mu molm^{-2}s^{-1}$ $\mu_{max} = 0.16h^{-1}$
Bechet et al. [74]			Indoor	*Chlorella vulgaris*	values are reported at six different temperatures in [74]
Kasiri et al. [75]			Indoor	*Chlorella kessleri*	$\mu_{max} = 0.73day^{-1}$ $K_I = 3.33\mu mol\ photonsm^{-2}s^{-1}$
Chalup and Laws [76] **and, Laws and Chalup** [77]	$\mu = \mu_{max}\frac{I}{I+K_I} - \mu_r$	(2)	Indoor	*Pavlova lutheri*	$\mu_{max} = 1.95day^{-1}$ $K_I = 10.8mol\ quantam^{-2}day^{-1}$
Smith [39]	$P = P_{max}\left(\frac{I^2}{I^2+K_I^2}\right)^{1/2}$	(3)	indoor	Gigartina harveyana	$\mu_r = 0.03day^{-1}$
Bannister [40]	$\mu = \mu_{max}\frac{I}{(I^m+K_I^m)^{1/m}}$	(4)	Indoor	*Chlorella pyrenoidosa*	$\mu_{max} = 2.48day^{-1}$ $m = 1.8$ $K_I = 5.7\mu Em^{-2}s^{-1}$
Lee et al. [33]	$\mu_{ave} = \mu_{max}\frac{I_{ave}}{(I_{ave}^m+K_I^m)^{1/m}}$	(5)	Indoor	*Spirulina platensis*	$\mu_{max} = 0.2976(h^{-1})$ $K_I = 15.01(W/m^2)$ $m = 0.4970$
Molina Grima et al. [78]	$\mu = \mu_{max}\frac{I^m}{I^m+K_I^m}$	(6)	Indoor	*Isochrysis galbana*	$\mu_{max} = 0.0426(h^{-1})$ $K_I = 10.92(W.m^{-2})$ $m = 5.13$
Molina Grima et al. [28]			Indoor	*Isochrysis galbana*	$\mu_{max} = 0.046(h^{-1})$ $K_I = 9.67\times10^{15}(quanta\ cm^{-2})m = 1.7$
Molina Grima et al. [59]			Indoor	*Isochrysis galbana*	*at* $820\mu Em^{-2}s^{-1}$ $\mu_{max} = 0.0465h^{-1}$ $K_I = 195.6\mu Em^{-2}s^{-1}$ $m = 2.11$ *at* $1630\mu Em^{-2}s^{-1}$ $\mu_{max} = 0.0448h^{-1}$ $K_I = 140.6\mu Em^{-2}s^{-1}$ $m = 1.58$ *at* $3270\mu Em^{-2}s^{-1}$ $\mu_{max} = 0.0459h^{-1}$ $K_I = 808.2\mu Em^{-2}s^{-1}$ $m = 0.98$

(*continued on next page*)

Table 1 (*continued*)

Source	Formula		System	Alga	Parameters
Concas et al. [79]			Indoor	*Spirulina platensis*	$\mu_{max} = 2.06\times10^{-5}(s^{-1})$ $K_I = 160\mu Em^{-2}s^{-1}$ $m = 1.49$
Pegallapati and Nirmalakhandan [80]			Indoor	*Nannochloropsis salina*	$\mu_{max} = 1.2(day^{-1})$ $K_I = 181\mu Em^{-2}s^{-1}$ $m = 1.75$
				Scenedesmus sp.	$\mu_{max} = 1.4(day^{-1})$ $K_I = 131\mu Em^{-2}s^{-1}$ $m = 2.7$
Fernandez et al. [81]			Outdoor light	*Scenedesmus almeriensis*	$K_I = 69\mu Em^{-2}s^{-1}$ $m = 0.87$
Costache et al. [82]	$P = P_{max}\frac{I^m}{I^m+(K_I\exp(k_eI))^m}$	(7)	Indoor	*Scendesmus almeriensis*	$m = 1.19$ $P_{max} = 4.6\times10^{-5}$ $(molO_2.gbiomass^{-1}min^{-1})$ $k_e = 1.85\times10^{-3}m^2s\mu E^{-1}$ $K_I = 76.35\mu Em^{-2}s^{-1}$
Fernandez et al. [83]			Outdoor	*Scenedesmus almeriensis*	$K_I = 139.3\mu Em^{-2}s^{-1}$ $k_e = 0.002m^2s\mu E^{-1}$ $m = 1.045$
Molina Grima [59]	$\mu = \mu_{max}\frac{I^{m_{app}}}{I^{m_{app}}+K_{app}^{m_{app}}}$ $m_{app} = \frac{n_2}{I_0}$ $K_{app} = I_K + \left(\frac{I_0}{K_I}\right)^{n_1}$	(8)	Indoor	*Isochrysis galbana*	$\mu_{max} = 0.0444(h^{-1})$ $I_K = 170.68(\mu Em^{-2}s^{-1})$ $K_I = 2217.2(\mu Em^{-2}s^{-1})$ $n_1 = 12.8$ $n_2 = 2728.8(\mu Em^{-2}s^{-1})$
Garcia-Malea et al. [60]	$\mu = \mu_{max}\frac{I^{m_{app}}}{I^{m_{app}}+K_{app}^{m_{app}}}$ $m_{app} = a + bI_0$ $K_{app} = c + dI_0$	(9)	indoor	*Haematococcus pluvialis*	$\mu_{max} = 0.11h^{-1}$ $a = 2.32$ $b = -0.00008(\mu Em^{-2}s^{-1})^{-1}$ $c = 98.7\mu Em^{-2}s^{-1}$ $d = 0.034$
Aiba [34]	$P = P_{max}\frac{I}{I+K_I+\frac{I^2}{K_i}}$	(10)	–	–	
Megard et al. [55]			Indoor	Various species	
Lee et al. [33]			Indoor vessel	*Spirulina platensis*	$\mu_{max} = 5.4849(h^{-1})$ $K_I = 959.2(W/m^2)$ $K_i = 0.5817(m^2/W)$
Molina Grima et al. [59]			Indoor	*Isochrysis galbana*	*at* $820\mu Em^{-2}s^{-1}$ $\mu_{max} = 0.1088h^{-1}$ $K_I = 195.1\mu Em^{-2}s^{-1}$ $K_i = \infty$ *at* $1630\mu Em^{-2}s^{-1}$ $\mu_{max} = 0.0513h^{-1}$ $K_I = 145.2\mu Em^{-2}s^{-1}$ $K_i = \infty$ *at* $3270\mu Em^{-2}s^{-1}$ $\mu_{max} = 0.0449h^{-1}$ $K_I = 697.2\mu Em^{-2}s^{-1}$ $K_i = \infty$
Fouchardet al. [84]			indoor	*Chlamydomonas reinhardtii*	$\mu_{max} = 0.2274h^{-1}$ $K_I = 81.38\mu mol\ photonm^{-2}s^{-1}$ $K_i = 2500\mu mol\ photonm^{-2}s^{-1}$
Ippoliti et al. [12]			Indoor and outdoor	*Isochrysis galbana*	$P_{max} = 1075mgO_2(g\ biomass.\ h)^{-1}$ $K_I = 311.8\mu Em^{-2}s^{-1}$ $K_i = 1253\mu Em^{-2}s^{-1}$
Concas et al. [3]	$\mu = \mu_{max}\frac{I}{I+K_I+\frac{I^2}{K_i}}$	(11)	Indoor	Nannochloris eucaryotum	$K_I = 60\mu Em^{-2}s^{-1}$ $K_i = 130\mu Em^{-2}s^{-1}$
Mirzaie et al. [85]			Indoor	*Chlorella vulgaris*	$K_I = 1.56\mu mol\ photonsm^{-2}s^{-1}$ $K_i = 15.42\mu mol\ photonsm^{-2}s^{-1}$
Peeters [54]	$\mu = \mu_{max}(1+\beta_I).\frac{2x_I}{x_I^2+2\beta_I x_I+1}$ $x_I = \frac{I}{I_{opt}}$	(12)			
Dauta et al. [58]			indoor	*Chlorella Vulgaris*	$\mu_{max} = 1.3day^{-1}$ $I_{opt} = 140\mu Em^{-2}s^{-1}$

(*continued on next page*)

Table 1 (*continued*)

Source	Formula		System	Alga	Parameters
				Fragilaria crotonensis	$\mu_{max} = 0.58 day^{-1}$ $I_{opt} = 150 \mu E m^{-2} s^{-1}$
				Straurastrum pingue	$\mu_{max} = 0.77 day^{-1}$ $I_{opt} = 270 \mu E m^{-2} s^{-1}$
				Synechocystis minima	$\mu_{max} = 1.32 day^{-1}$ $I_{opt} = 125 \mu E m^{-2} s^{-1}$
Talbot et al. [86]	$\mu = \mu_{max}(1+\beta_I).\frac{2x_I}{x_I^2+2\beta_I x_I+1}$ $x_I = \frac{I}{I_{opt}}$ $y = \mu_{max}$, I_{opt},or β $y = y_{max}\left(\frac{T}{\theta_{opt}} w^u\right)^{\alpha}$ $w = \frac{\theta_0 - T}{\theta_0 - \theta_{opt}}$ $u = \frac{\theta_0 - \theta_{opt}}{\theta_{opt}}$	(13)	indoor	*Oscillatoria agardhii*	I_{opt}: $y_{max} = 101 \mu E m^{-2} s^{-1}$ $\theta_{opt} = 24°C, \theta_0 = 43°C$, $\alpha = 1.6$ μ_{max}: $y_{max} = 0.5 day^{-1}, \theta_{opt} = 37°C$ $\theta_0 = 43°C$, $\alpha = 0.3$ β: $y_{max} = 2.3, \theta_{opt} = 18°C$ $\theta_0 = 43°C$, $\alpha = 1.9$
				Ankistrodesmus falcatus	I_{opt}: $y_{max} = 174 \mu E m^{-2} s^{-1}$ $\theta_{opt} = 29°C, \theta_0 = 43°C$, $\alpha = 1.2$ μ_{max}: $y_{max} = 1.1 day^{-1}, \theta_{opt} = 37°C$ $\theta_0 = 43°C$, $\alpha = 0.2$ β: $y_{max} = 2.2, \theta_{opt} = 22°C$ $\theta_0 = 43°C$, $\alpha = 1.5$
				Phormidiumbohneri	I_{opt}: $y_{max} = 541 \mu E m^{-2} s^{-1}$ $\theta_{opt} = 30°C, \theta_0 = 43°C$, $\alpha = 4.8$ μ_{max}: $y_{max} = 1.7 day^{-1}, \theta_{opt} = 37°C$ $\theta_0 = 43°C$, $\alpha = 2.7$ β: $y_{max} = 5.4, \theta_{opt} = 23°C$ $\theta_0 = 43°C$, $\alpha = 5$
Dermoun et al. [87]	$\mu = \mu_{max}(1+\beta_I).\frac{2x_I}{x_I^2+2\beta_I x_I+1}$ $x_I = \frac{I}{I_{opt}}$ $\mu_{max}(T) = \gamma(1+\beta_T^g).\frac{2x_g}{x_g^2+2\beta_{T,g} x_g+1}$ $x_g = \frac{T-\theta_{g,0}}{\theta_{g,opt}-\theta_{g,0}}$ $I_{opt}(T) = \rho_I(1+\beta_{T,I}).\frac{2x_{T,I}}{x_{T,I}^2+2\beta_{T,I}x_{T,I}+1}$ $x_{T,I} = \frac{T-\theta_{I,0}}{\theta_{I,opt}-\theta_{I,0}}$	(14)	Indoor	*Pophyridium cruentum*	$\beta_I = 0.5$ $\rho_I = 538(\mu mol\ photon m^{-2} s^{-1})$ $\beta_{T,I} = 0.56$ $\theta_{I,0} = 4.7(°C)$ $\theta_{I,opt} = 12.3(°C)$ $\gamma = 1.4(day^{-1})$ $\beta_{T,g} = 0.02$ $\theta_{g,0} = 4.7(°C)$ $\theta_{g,opt} = 20.5(°C)$
Grobbelaar [88]	$\mu = \mu_m(T).\frac{I}{I+K_I(T)}(1-\alpha(T).I) - r(T)$ $\mu_m = \mu_0 \theta_{\mu}^{\frac{T-10}{10}}$ $K_I = K_{I0}\theta_K^{\frac{T-10}{10}}$ $\alpha = \alpha_0 \theta_{\alpha}^{\frac{T-10}{10}}$ $r(T) = r_0 \theta_r^{\frac{T-10}{10}} - r_1$	(15)	Outdoor	*Scendesmus obliquus, Coelastrum sphaericum*	
Lee et al. [33]	$\mu_{ave} = \frac{I_{ave}}{K_1 + K_2 I_{ave}^2}$	(16)	Indoor vessel	*Spirulina platensis*	$K_1 = 177.9(W/m^2/h)$ $K_2 = 0.1083(m^2/h/W)$
Bernard and Remond [15]	$\mu = \mu_{max}\frac{I}{I+\frac{\mu_{max}}{\alpha}\left(\frac{I}{I_{opt}}-1\right)^2}$	(17)		*Nannochloropsis oceanica*	$\mu_{max} = 2 day^{-1}$ $\alpha = 0.05 \mu E^{-1} m^2 s\ day^{-1}$ $I_{opt} = 275 \mu E m^{-2} s^{-1}$
				Chlorella pyrnoidosa	$\mu_{max} = 1.85 day^{-1}$ $\alpha = 0.12 day^{-1}$ $I_{opt} = 2.03 \times 10^8 \mu E m^{-2} s^{-1}$

(*continued on next page*)

Table 1 (*continued*)

Source	Formula		System	Alga	Parameters
Munoz-Tamayo et al. [89]				*Tisochrysis lutea*	$\mu_{max} = 0.76 day^{-1}$ $\alpha = 0.008 \mu E^{-1} m^2 s\ day^{-1}$ $I_{opt} = 548 \mu E m^{-2} s^{-1}$
Ogbonna et al. [90]	$\mu = K\left(\frac{Ia}{X.V} - r_m(1-V_F)\right)$	(18)	Indoor	*Chlorella pyrenoidosa*	$V = 0.75L$ $X_0 = 0.01905 kg.m^{-3}$ $K = 0.8 kg.\ mol^{-1}$ $r_m = 0.13 mol.kg^{-1}$
Lee et al. [33]	$\mu_{ave} = aI_{ave} + b$	(19)	Indoor vessel	*Spirulina platensis*	$a = 0.0023 (m^2/W/h)$ $b = 0.0254 (h^{-1})$
Van Oorschot [49] **a.k.a. Poisson model**	$P = P_{max}\left(1-\exp\left(-\frac{\alpha I}{P_{max}}\right)\right)$ *or* $P = P_{max}\left(1-\exp\left(-\frac{I}{K_I}\right)\right)$	(20)			
Molina Grima et al. [59]			Indoor	*Isochrysis galbana*	*at* $820 \mu E m^{-2} s^{-1}$ $\mu_{max} = 0.064 h^{-1}$ $K_I = 456.8 \mu E m^{-2} s^{-1}$ *at* $1630 \mu E m^{-2} s^{-1}$ $\mu_{max} = 0.043 h^{-1}$ $K_I = 195.2 \mu E m^{-2} s^{-1}$ *at* $3270 \mu E m^{-2} s^{-1}$ $\mu_{max} = 0.034 h^{-1}$ $K_I = 724.7 \mu E m^{-2} s^{-1}$
Geider et al. [91]			Indoor	Various species	Parameters can be found in [91]
Geider et al. [92]			Indoor	*Thalassiosira psedonana*	$\alpha = 1 \times 10^{-5} g\ Cm^{-2} (g\ Chl\ a \mu mol\ photons)^{-1} \mu_{max} = 5.1 day^{-1}$
				Pavlova lutheri	$\alpha = 0.46 \times 10^{-5} g\ Cm^{-2} (g\ Chl\ a \mu mol\ photons)^{-1} \mu_{max} = 3 day^{-1}$
				Skeletonema costatum	$\alpha = 1.38 g\ Cm^{-2} (g\ Chl\ a \mu mol\ photons)^{-1} \mu_{max} = 3 day^{-1}$
				Isochrysis galbana	$\alpha = 0.46 g\ Cm^{-2} (g\ Chl\ a \mu mol\ photons)^{-1} \mu_{max} = 3 day^{-1}$
Meseck et al. [93]			Indoor	*Tetraselmis chui*	$\mu_{max} = 0.77 day^{-1}$ $K_I = 7.14 Em^{-2} day^{-1}$
Bechet et al. [74]			Indoor	*Chlorella vulgaris*	
Steele [52]	$P = P_{max}.\ \frac{I}{I_{opt}} e^{1-I/I_{opt}}$	(21)	Outdoor	Sea phytoplanktons	
Molina Grima et al. [59]			Indoor	*Isochrysis galbana*	*at* $820 \mu E m^{-2} s^{-1}$ $\mu_{max} = 0.0521 h^{-1}$ $I_{opt} = 1020.3 \mu E m^{-2} s^{-1}$ *at* $1630 \mu E m^{-2} s^{-1}$ $\mu_{max} = 0.0484 h^{-1}$ $I_{opt} = 741.9 \mu E m^{-2} s^{-1}$ *at* $3270 \mu E m^{-2} s^{-1}$ $\mu_{max} = 0.32 h^{-1}$ $I_{opt} = 2217.9 \mu E m^{-2} s^{-1}$
Baquerisse et al. [94]			Indoor	*Porphyridim purpureum*	
James and Boriah [95]			Indoor	*Phaeodactylum tricornutum*	
Marsullo et al. [96]			Indoor	*Phaeodactylum tricornutum*	$\mu_{max} = 1.392 day^{-1}$ $I_{opt} = 37.118 Wm^{-2}$
				Thalassiosira pseuinana	$\mu_{max} = 3.288 day^{-1}$ $I_{opt} = 21.834 Wm^{-2}$
Chalker [48]	$P = P_{max} \tanh(\alpha I)$	(22)	Indoor	*Gymnodinium microadriaticum*	$P_{max} = 36 mol O_2 h^{-1} (mol\ Chl\ a)^{-1}$ $\alpha = 4.6 E^{-1} m^2 h$
Bechet et al. [74]			Indoor	*Chlorella vulgaris*	
Lee and Zhang [76]			Indoor	*Chlorella* sp.	$\alpha = 0.0590 \mu mol\ photon^{-1} m^2 s$
Collins and Boylen [97]	$\mu = \mu_{max}(T)\frac{I}{I + K_I(T)} - r(T)$ $\mu_{max} = \mu_0 e^{k_\mu T}$ $K_I(T) = K_{I0} e^{k_K T}$ $r = r_0 e^{k_r T}$	(23)	Indoor	*Anabaena variabilis*	$\mu_0 = 0.098\left(\frac{gC}{gDW} day^{-1}\right)$ $k_\mu = 0.0854 (°C^{-1})$ $K_{I0} = 32.05\left(\frac{\mu E}{m^2 s}\right)$ $k_K = 0.078 (°C^{-1})$ $r0 = 0.072\left(\frac{gC}{gDW} day^{-1}\right)$ $k_r = 0.067 (°C^{-1})$

(*continued on next page*)

Table 1 (*continued*)

Source	Formula		System	Alga	Parameters
Guterman [98]	$\mu = \mu_p - r$ $\mu_p = qI\left(\frac{1-(T-T_{opt})^2}{\Delta T^2}\right)$ $r = (aT + b).\frac{zD}{H}$	(24)	Outdoor	*Spirulina platensis*	$q = 5.679 min^{-1} klux^{-1}$ $T_{opt} = 33°C$ $\Delta T = 25°C$ $a = -0.231 min^{-1} °C^{-1}$ $b = 0.343 min^{-1}$
Carvalho and Malcata [99]	$\mu = \mu_{max}\left(1-\frac{X}{X_{max}}\right)$ $\mu_{max} = \frac{K_1 I}{K_2 T + I} e^{-\frac{K_3 I}{RT}}$	(25)	indoor	*Pavlova lutheri*	$K_1 = -2.72 day^{-1}$ $K_2 = -2.86°C^{-1}$ $K_3 = 129\times10^2 J.\ mol^{-1}$
Muller-Feuga [100]	$\mu = \mu_{max}\frac{2(1-\rho_e)(\rho-\rho_e)}{(1-\rho_e)^2+(\rho-\rho_e)^2}$ $\rho = \frac{I}{I_{opt}}, \rho_e = \frac{I_e}{I_{opt}}$	(26)	Indoor	*Pophyridium cruentum*	$\mu_{max} = 1.06 day^{-1}$ $I_{opt} = 485 \mu mol\ photon m^{-2} s^{-1}$ $I_e = 42 \mu mol\ photon m^{-2} s^{-1}$
Lee and Zhang [76]			Indoor	*Chlorella* sp.	$I_{opt} = 54$ μmol photon m^{-2} s^{-1} $I_e = 1$ μmol photon m^{-2} s^{-1} $\mu_{max} = 0.7 day^{-1}$
Rubio Camacho et al. [63]	$x_e^* = \frac{1}{2}\left(\left(1-\kappa-\frac{\alpha_I}{I}\right)+\sqrt{\left(1-\kappa-\frac{\alpha_I}{I}\right)^2+4\kappa}\right)$ Light limited: $\frac{\mu}{\mu_{max}} = \frac{I}{\alpha_I}(1-x_e^*)$ Photoinhibited: $\kappa = \kappa_I(1+\delta\sqrt{I})$ $\alpha_I = \alpha_{I,I}(1+\delta\sqrt{I})$ $\frac{\mu}{\mu_{max}} = \frac{I}{\alpha_I}\frac{(1-x_e^*)}{1+\delta\sqrt{I}}$	(27)	Indoor	*Chlorella pyrenoidosa*	

due to the nature of the equation as it has low curvature and reaches the maximum value at a low pace.

Later, Smith [39] used a new model similar to Baly's model with some modifications. By substituting irradiance and saturation constant with the square of their value, the model reached a larger curvature and therefore made model closer in shape to a typical PI curve. Bannister et al. [40] employed the same idea but instead of using square values, they used power m of them (also referred to as shape factor) which enabled the model to adjust its curvature based on the experimental data. Using values 1 and 2 for m transforms the equation into Baly and Smith's models respectively; however, after testing the model on the data from various experiments [41–45] Bannister proposed that the value of m must be between 2 and 3.

Jassby and Platt [46,47] used data from 188 experiments on light saturation curve at Nova Scotia coastal waters and compared eight different models including the ones that were developed by Baly and Smith. After an extensive comparison, they concluded that a hyperbolic tangent function was the best fit to the experimental data. Chalker [48] performed a similar study and compared four different types of equations and confirmed that as Jassby and Platt [46] concluded the hyperbolic tangent function gives the best results. Bannister stated that hyperbolic tangent function closely matches his model when m is 2.5, which is consistent with the proposed limits for m [40].

Van Oorschot [49] used an exponential equation known as Poisson function to describe the effect of light. Although this model showed to be a better fit to experimental data than Baly's model, in the analysis by Jassby and Platt [46] it did not perform as good as hyperbolic tangent function.

So far all the equations suggest that as light intensity tends to infinity, the growth rate approaches its maximum value while this contradicts the experiment where after a certain intensity, the growth rate will drop again [50,51]. This effect known as photoinhibition needs to be reflected in the model as well. Therefore, Steel [52] proposed a model to describe this effect:

$$\mu = \mu_{max}.\ \frac{I}{I_{opt}} e^{1-\frac{I}{I_{opt}}} \tag{2}$$

In this model when the intensity reaches I_{opt}, the growth rate will be at its maximum value, and any increase in light intensity results in lower growth rate. However, Steele [52] reported that in the shallow cultures the amount of discrepancy was relatively high. Later, Crill [53] defined photosynthetic factories where light is trapped and initiates the photosynthetic reactions and by incorporating probability functions, the same formula as Steele's was derived.

Another equation later proposed by Aiba [34], Peeters and Eilers [54] and Megard et al. [55] added an inhibition term to Tamiya's equation:

$$\mu = \mu_{max}.\ \frac{I}{K_I + I + I^2/K_i} \tag{3}$$

Eilers and Peeters [56,57] improved Crill's model [53] and proposed a new model based on the dynamic study of photosynthesis. They assumed photosynthetic units (PSU) can experience three states: (1) resting state, (2) activated state, and (3) deactivated or damaged state. Then by defining the rate of state changes they managed to formulate the effect of light on photosynthesis at steady state conditions. Peeters and Eilers [54] also rearranged the model to show the effect of irradiance on photosynthesis based on optimum irradiance.

$$\mu = \mu_{max}(1+\beta_I).\ \frac{2x_I}{x_I^2+2\beta_I x_I+1} x_I = I/I_{opt} \tag{4}$$

Dauta et al. [58] compared Peeters and Eilers equation with Steels equation for four different microalgae species and found former to be more accurate. In a study Lee et al. [33] modified Aiba's equation to reduce the number of constants and facilitate parameter estimation.

$$\mu = \mu_{max}.\ \frac{I}{K_I + K_i.\ I^2} \tag{5}$$

Even though the above equation still seems to have three parameters, by introducing $K_1 = K_I/\mu_{max}$ and $K_2 = K_i/\mu_{max}$, the number of parameters will be reduced to two. They used experimental data for growth of *Spirulina platensis* and compared the new equation with the models by Baly [36], Bannister [40], and Aiba [34] and concluded that their model besides Aiba's are the only ones able to perform well at high

irradiance while their model had a smaller mean square deviation in general.

Molina Grima et al. [28] developed a model based on bannister's model using average intensity which later was enhanced by replacing the shape factor, m, and the photo-saturation constant, K_I, by apparent values which could be calculated using specific relations [59]:

$$\mu = \mu_{max} \cdot \frac{I_{ave}^{n_{app}}}{I_{app}^{n_{app}} + I_{ave}^{n_{app}}} \tag{6}$$

$$n_{app} = n_2/I \tag{7}$$

$$I_{app} = I_k + \left(\frac{I}{K_I}\right)^{n_1} \tag{8}$$

where n_1, n_2 are model constants.

They assumed that photoinhibition is caused by the damaged photosystem at a high light intensity which is the case only where the light enters the culture. Thus, due to light attenuation, photoinhibition does not happen in the depth of the culture as the light intensity drops significantly. On the other hand, regeneration of photosystem is not bounded by the cell location and can happen anywhere in the culture. Therefore, the growth rate should be related to both incident and average light intensity.

Another modification of Bannister's model was done by Garcia-Malea et al. [60] where the shape factor and the saturation constant were related linearly to irradiance at the surface:

$$\mu = \mu_{max} \cdot \frac{I_{av}^{a+bI_0}}{(c + dI_0)^{a+bI_0} + I_{av}^{a+bI_0}} \tag{9}$$

In 2000, Han et al. [35] argued that since microalgae experience variable irradiance, using static modelling is not the best approach. Therefore, they involved the dynamic aspect of light in the model to reach more accuracy. They used the same idea as Peeters and Eilers [54,56,57] but instead of simplifying the model for steady state condition, they kept the dynamic characteristics of the model. Due to consideration of light history of cells this model could potentially be valuable for hydrodynamic study of microalgal culture, where cells experience various light conditions [61,62]. It also enables the model to account for unique phenomenon in microalgae cultures known as flash light effect [63]. However, in this paper we have not reviewed dynamic models, as a summary of them can be found in Bechet et al. [51].

2.1.1. Light spectrum

Although light is one of the most important factors in the growth of microalgae, it is not only the intensity of light that is important but also its spectrum as well. Microalgae have been shown to grow in certain wavelengths of light better than the others, and thus some researchers studied this effect as well [30]. This light range, which is also known as photosynthetically active radiation (PAR), is responsible for providing energy for the reactions and its wavelength ranges from 400 nm to 700 nm [30]. Blanken et al. [27] took this effect into account and assumed the effective light intensity is caused by these wavelengths and considering light attenuation, he proposed a formula for light intensity inside the culture:

$$I(z) = \sum_{\lambda=400}^{700} I_\lambda(0) e^{a_x C_x z} \Delta\lambda \tag{10}$$

where $I_\lambda(0)$ is light intensity at surface for wavelength λ , a_x is light absorption rate, C_x is biomass concentration, and z is depth of the point at which light intensity is calculated.

Ritchie [64] made the range of effective wavelengths even narrower by considering only blue (425–500 nm) and red (640–700 nm) light. Using the results of McCree [65] he added average quantum efficiency and calculated photosynthetically useable radiation (PUR).

$$I_{PUR} \approx 0.668 \times \int_{425}^{500} I_\lambda d\lambda + 0.819 \times \int_{640}^{700} I_\lambda d\lambda \tag{11}$$

The highest solar irradiance on the surface of the earth can reach about 2220 μmol m^{-2} s^{-1}, of which , according to Eq. (11), only about 767 μmol m^{-2} s^{-1} can be used for photosynthesis [65]. The usable light intensity calculated in Eq. (11) may replace irradiance in most of the presented growth models.

Moreover, wavelengths out of PAR range do not stimulate growth but may have inhibitory effects. Studies show that UV irradiation can cause inhibition of photosynthesis and even death of algal cells and consequently limit growth rate [66–68].

2.2. Nutrients

Microalgae require various nutrients for growth and when they undergo nutrient limitation the growth can be affected significantly. Nitrogen and phosphorus compounds play an important role on the growth and the organic composition of algal cells [101,102]. There are also many micronutrients such as cobalt, iron, molybdenum, and manganese, which are necessary for optimum growth of microalgae [103]. Many models have been used to explain the effect of nutrients on the growth of microalgae, a summary of which can be found in Table 2. Monod [38] introduced one of the first growth models which was initially intended for bacterial cultures but later was used by many researchers for algal cultures as well. He tried to study the biochemistry of bacteria using bacterial growth where he just limited the study to positive growth and neglected the death rate. He used a Michaelis-Menten equation to describe the growth rate as a function of the concentration of nutrient.

$$\mu = \mu_{max} \frac{S}{K_s + S} \tag{12}$$

Where μ is specific growth rate, μ_{max} is maximum specific growth rate, S is concentration of the limiting nutrient, and K_s is concentration of limiting nutrient at which the specific growth rate is half of its maximum value.

Many studies used this model as a basis and found the parameters of this model for their specific alga type [104–107]. Goldman et al. [104] divided the growth based on the concentration of limiting nutrient into three areas. The first area is the low concentration of nutrient which is defined as a concentration in which specific growth rate is less than half of its maximum value. In this area, the specific growth rate is in a linear relationship with limiting nutrient concentration.

$$\mu = \mu_{max} \cdot \frac{S}{K_S} \tag{13}$$

The second area is where Monod equation applies till when the specific growth rate is almost reached the maximum value. The third area is the constant growth rate area where based on Monod equation given $K_S \ll S$ then $\mu = \mu_{max}$ and further increase in concentration will not result in any change in the specific growth rate.

Despite its popularity among researchers, Monod equation failed when high concentration of nutrients had negative effect on growth. Andrews [108] used Monod equation and performed some modifications to add the inhibitory effect of high concentrations which may be significant during transient conditions like system start-up. For this purpose he added an inhibitory term to the equation:

$$\mu = \mu_{max} \cdot \frac{S}{S + K_s + \frac{S^2}{K_i}} \tag{14}$$

where K_i is inhibition constant and μ_{max} is a theoretical value representing maximum specific growth rate if there was no inhibition. Andrews pointed out that this equation does not follow a theoretical basis and is empirically derived and lacks the effects of organism death, inhibitory effect of products, and delayed response of microalgae to

Table 2
Models considering effect of nutrients.

Source	Model		System	Alga type	Estimation
Monod [38]	$\mu = \mu_{max}\frac{S}{K_S+S}$	(1)			
Haario et al. [70]			Outdoor	Diatom	$\mu_{max} = 0.0886\ day^{-1}$ *N:* $K_S = 14.5\ (\mu g/L)$ *P:* $K_S = 10.4\ (\mu g/L)$
				Chrysophycea	$\mu_{max} = 0.0465\ day^{-1}$ *N:* $K_S = 32.9\ (\mu g/L)$ *P:* $K_S = 8.27\ (\mu g/L)$
				Cyanobacteria	$\mu_{max} = 0.329\ day^{-1}$ *N:* $K_S = 21\ (\mu g/L)$ *P:* $K_S = 5.5\ (\mu g/L)$
				Minor species	$\mu_{max} = 0.212\ day^{-1}$ *N:* $K_S = 45.7\ (\mu g/L)$ *P:* $K_S = 77.3\ (\mu g/L)$
Xin et al. [107]				*Scenedesmus* sp.	$N{:}K_S = 12.1\ mg\ L^{-1}$ $P{:}K_S = 0.27\ mg\ L^{-1}$
Concas et al. [79]			Indoor	Spirulina platensis	$N{:}K_S = 5.314\ g\ m^{-3}$ $P{:}K_S = 0.028 gm^{-3}$
Spijkerman et al. [129]			Indoor	Chlamydomonas acidophila	Multiplicative model: $\mu_{max} = 0.073h^{-1}$ C: $K_S = 0.38\mu M$ P: $K_S = 1.09nM$ Threshold model: $\mu_{max} = 0.076h^{-1}$ C: $K_S = 1.43\mu M$ P: $K_S = 1.46nM$
Jayaraman and Rhinehart [18]				*Gladieria sulphuraria*	
Chen et al. [130]				*Micrpcystis aeruginosa*	$P{:}K_S = 0.025(mgL^{-1})$
Marsullo et al. [96]			Indoor	*Phaeodactylum tricornutum*	N: $K_S = 0.001 mol.m^{-3}$
				Thalassiosira pseuinana	N: $K_S = 0.001 mol.m^{-3}$
Lee and Zhang [76]				*Chlorella* sp.	$N{:}K_S = 0.1 mgL^{-1}$
Concas et al. [3]			Indoor	Nannochloris eucaryotum	$N{:}K_S = 5.4\times10^{-4} gL^{-1}$ $P{:}K_S = 2.5\times10^{-5} gL^{-1}$
Fre et al. [131]			Indoor	*Dunaliella tertiolecta*	$75 mgL^{-1}$ of sodium nitrate $\mu_{max} = 0.02790h^{-1}$ $K_S = 0.9\times10^{-4} g.L^{-1}$ $300 mgL^{-1}$ of sodium nitrate $\mu_{max} = 0.02804h^{-1}$ $K_S = 8.52\times10^{-4} g.L^{-1}$ $600 mgL^{-1}$ of sodium nitrate $\mu_{max} = 0.02567h^{-1}$ $K_S = 2.374\times10^{-3} g.L^{-1}$ $900 mgL^{-1}$ of sodium nitrate $\mu_{max} = 0.02617h^{-1}$ $K_S = 3.944\times10^{-3} g.L^{-1}$
Martinez Sancho et al. [112] **and Martinez et al.** [113]	$\mu = \frac{\mu_{m1}S+\mu_{m2}K_S}{K_S+S}$	(2)		*Scenedesmus obliquus*	$\mu_{m1} = 0.0466h^{-1}$ $\mu_{m2} = 0.0256h^{-1}$ $K_S = 0.2\mu M$
Martinez et al. [113]	$\mu = \frac{\mu_{m1}K_I S+\mu_{m2}S^2+\mu_{m3}K_S K_I}{K_S K_I + K_I S + S^2}$	(3)		*Scenedesmus obliquus*	Values at different temperatures are reported in [113]
Andrews [108]	$\mu = \mu_{max}\frac{S}{K_S+S+S^2/K_{iS}}$	(4)			
Zhang et al. [132]			Indoor	*Chlamydomonas reinhardtii*	For nitrate: $K_S = 2.6085 g.L^{-1}$ $K_{iS} = 0.1065 g.L^{-1}$ For ammonium chloride: $K_S = 2.2956 g.L^{-1}$ $K_{iS} = 0.1557 g.L^{-1}$ For urea: $K_S = 2.3978 g.L^{-1}$ $K_{iS} = 0.0708 g.L^{-1}$
Kasiri et al. [75]			Indoor	*Chlorella kessleri*	$\mu_{max} = 0.73 day^{-1}$ $K_S = 722 mgL^{-1}$ $K_i = 1.28\times10^4 mgL^{-1}$

(*continued on next page*)

Table 2 (*continued*)

Source	Model		System	Alga type	Estimation
Mirzaie et al. [85]			Indoor	*Chlorella vulgaris*	$\mu_{max} = 0.13 day^{-1}$ $K_S = 0.117 g.L^{-1}$ $K_{iS} = 0.073 g.L^{-1}$
Lee and Zhang [76]			Indoor	*Chlorella* sp.	$N{:}K_S = 1.78 mgL^{-1}$ $K_{iS} = 364 mgL^{-1}$
Spijkerman et al. [129][a]	$\mu = \mu_{max}\frac{C}{K_C + C}$ $K_C = \frac{\mu_{max}}{\alpha_{Cmax}} \times \frac{K_P + P}{P}$	(5)	Indoor	Chlamydomonas acidophila	$\mu_{max} = 0.059 h^{-1}$ $K_P = 0.7 nM$ $\alpha_{Cmax} = 0.039$
Spijkerman et al. [129][a]	$\mu = \mu_{max}\frac{P}{K_P + P}$ $K_P = \frac{\mu_{max}}{\alpha_{Pmax}} \times \frac{K_C + C}{C}$	(6)	Indoor	Chlamydomonas acidophila	$\mu_{max} = 0.066 h^{-1}$ $K_C = 0.77 \mu M$ $\alpha_{Pmax} = 0.075$
Droop [110]	$\mu = \mu'_{max}\left(1 - \frac{Q_{min}}{Q}\right)$	(7)		*Monochrysis lutheri*	
Burmaster [133]				*Monochrysis lutheri*	$\mu_{max} = 1.03 (day^{-1})$ $Q_{min} = 7.02 \times 10^{-16} mol.\ cell^{-1}$
Packer et al. [29]			Indoor	*Pseudochlorococcum* sp.	$\mu_{max} = 3.26 day^{-1}$ $Q_{min} = 0.0278 gN.(g\ dw)^{-1}$
Wu et al. [134]			Indoor	*Scenedesmus* sp.	$\mu_{max} = 0.34 day^{-1}$ $Q_{min} = 0.019\%$
Fre et al. [131]			Indoor	*Dunaliella tertiolecta*	$75 mgL^{-1}$ of sodium nitrate $\mu_{max} = 0.04669 h^{-1}$ $Q_{min} = 0.02634 mg.g^{-1}$ $300 mgL^{-1}$ of sodium nitrate $\mu_{max} = 0.04319 h^{-1}$ $Q_{min} = 0.03505 mg.g^{-1}$ $600 mgL^{-1}$ of sodium nitrate $\mu_{max} = 0.05289 h^{-1}$ $Q_{min} = 0.08543 mg.g^{-1}$ $900 mgL^{-1}$ of sodium nitrate $\mu_{max} = 0.04628 h^{-1}$ $Q_{min} = 0.1179 mg.g^{-1}$
Guest et al. [126]	$\mu = \mu'_{max}\left(1 - \left(\frac{Q_{min}}{Q}\right)^4\right)$	(8)	Indoor	*Chalmydomonas reinhardtii*	
Geider [92]	$\mu = \mu'_{max}\left(\frac{Q - Q_{min}}{Q_{max} - Q_{min}}\right)$	(9)	Indoor	*Thalassiosira psedonana*	$Q_{min} = 0.04\left(\frac{g\,N}{g\,C}\right)$ $Q_{max} = 0.2\left(\frac{g\,N}{g\,C}\right)$
				Pavlova lutheri	$Q_{min} = 0.04\left(\frac{g\,N}{g\,C}\right)$ $Q_{max} = 0.2\left(\frac{g\,N}{g\,C}\right)$
				Skeletonema costatum	$Q_{min} = 0.04\left(\frac{g\,N}{g\,C}\right)$ $Q_{max} = 0.2\left(\frac{g\,N}{g\,C}\right)$
				Isochrysis galbana	$Q_{min} = 0.04\left(\frac{g\,N}{g\,C}\right)$ $Q_{max} = 0.167\left(\frac{g\,N}{g\,C}\right)$
Caperon and Meyer [122,123]	$\mu = \mu'_{max}\frac{Q - Q_{min}}{K_C + Q - Q_{min}}$	(10)		*Coccochloris*	$\mu_{max} = 0.090 (h^{-1})$ $Q_{min} = 0.075\left(\frac{mol\,N}{mol\,C}\right)$ $K = 0.057\left(\frac{mol\,N}{mol\,C}\right)$
				Cyclotella	$\mu_{max} = 0.087 (h^{-1})$ $Q_{min} = 0.043\left(\frac{mol\,N}{mol\,C}\right)$ $K = 0.053\left(\frac{mol\,N}{mol\,C}\right)$
				Dunaliella	$\mu_{max} = 0.076 (h^{-1})$ $Q_{min} = 0.044\left(\frac{mol\,N}{mol\,C}\right)$ $K = 0.034\left(\frac{mol\,N}{mol\,C}\right)$
Flynn [111]	$\mu = \mu'_{max}\frac{\hat{Q}(1 + k_Q)}{\hat{Q} + k_Q}$ $\hat{Q} = \frac{Q - Q_{min}}{Q_{max} - Q_{min}}$	(11)			

(*continued on next page*)

Table 2 (*continued*)

Source	Model		System	Alga type	Estimation
Chapelle et al. [135]				*Alexandrium minutum*	$\mu_{max} = 0.55 day^{-1}$ $Q_{min} = 3.7 pg.\ cell^{-1}$ $Q_{max} = 32.6 pg.\ cell^{-1}$ $K_Q = 4.24$
				Heterocapsa triquetra	$\mu_{max} = 0.67 day^{-1}$ $Q_{min} = 5.5 pg.\ cell^{-1}$ $Q_{max} = 15.6 pg.\ cell^{-1}$ $K_Q = 1.34$
Bougaran et al. [120]	$\mu = \mu'_{max} \frac{\left(1 - \frac{Q_{min}}{Q}\right)}{\left(1 - \frac{Q_{min}}{Q_{max}}\right)}$	(12)	Indoor	*Selenastrum minutum*	$\mu_{max} = 1.58 (day^{-1})$ N: $Q_{min} = 0.06\left(\frac{mol\ N}{mol\ C}\right)$ $Q_{max} = 0.21\left(\frac{mol\ N}{mol\ C}\right)$ P: $Q_{min} = 0.0018\left(\frac{mol\ N}{mol\ C}\right)$ $Q_{max} = 0.015\left(\frac{mol\ N}{mol\ C}\right)$
				Isochrysis affinis galbana	$\mu_{max} = 1.5 (day^{-1})$ N: $Q_{min} = 0.065\left(\frac{mol\ N}{mol\ C}\right)$ $Q_{max} = 0.14\left(\frac{mol\ N}{mol\ C}\right)$ P: $Q_{min} = 0.0009\left(\frac{mol\ N}{mol\ C}\right)$ $Q_{max} = 0.006\left(\frac{mol\ N}{mol\ C}\right)$
Fouchardet al. [84]	$\frac{\mu}{\mu'_{max}} = f(Q)$ $\frac{f(Q) - f_{min}}{1 - f_{min}} = \frac{\exp\left(k.\frac{Q}{Q_m}\right) - 1}{\exp(k) - 1}$	(13)	indoor	*Chlamydomonas reinhardtii*	$Q_m = 7 mg\ Sulfur\ (mg\ biomass)^{-1} k = 0.3389$ $f_{min} = 0.0674$
De La Hoz Siegler et al. [136,137][b,c]	$\mu = \mu'_{max} \frac{\tilde{q}}{K_q + \tilde{q}} \exp\left(-\frac{\bar{q}}{K_i}\right)$ $\bar{q} = \frac{1}{t} \int_0^t \tilde{q}\, dt$ $\tilde{q} = \frac{Q}{X + L + Q}$	(14)	Indoor	*Auxenochlorella protothecoides*	$\mu_{max} = 11.12 day^{-1}$ $K_q = 0.0022$ $K_i = 0.016$
Abdollahi and Dubljevic [138]			Indoor	*Auxenochlorella protothecoides*	$\mu_m = 14.18 day^{-1}$ $K_q = 0.0041$ $K_i = 0.016$
He et al. [139][c]	$\mu = \mu_{max}\left(1 - \frac{X}{X_{max}}\right)$	(15)	Indoor	*Isochrysis galbana*	N: 25 mg of sodium nitrate $\mu_{max} = 0.721 day^{-1}$ $X_{max} = 387.9 mgL^{-1}$ 50 mg of sodium nitrate $\mu_{max} = 0.568 day^{-1}$ $X_{max} = 538.28 mgL^{-1}$ 75 mg of sodium nitrate $\mu_{max} = 0.448 day^{-1}$ $X_{max} = 670.58 mgL^{-1}$ 100 mg of sodium nitrate $\mu_{max} = 0.416 day^{-1}$ $X_{max} = 835.41 mgL^{-1}$
Tavatia et al. [140][c]	$\mu = \mu_{max} \alpha(t)\left(1 - \frac{X}{X_{max}}\right)$ $\alpha(t) = \frac{e^{-h_0}}{e^{-\mu_{max} t} + e^{-h_0} - e^{-\mu_{max} t - h_0}}$	(16)			Reported in [140] for various ammonium concentrations

(*continued on next page*)

Table 2 (*continued*)

Source	Model		System	Alga type	Estimation
Fre et al. [131][c]	$\mu = \mu_{max}\left(\frac{S}{K_S+S}\right)\left(\frac{K_X}{X+K_X}\right)$	(17)	Indoor	*Dunaliella tertiolecta*	$300 mgL^{-1}$ of sodium nitrate $\mu_{max} = 0.02858h^{-1}$ $K_S = 5.05\times10^{-4} g.L^{-1}$ $K_X = 5.474 g.L^{-1}$ $600 mgL^{-1}$ of sodium nitrate $\mu_{max} = 0.02889h^{-1}$ $K_S = 5.232\times10^{-3} g.L^{-1}$ $K_X = 3.958 g.L^{-1}$ $900 mgL^{-1}$ of sodium nitrate $\mu_{max} = 0.02870h^{-1}$ $K_S = 5.851\times10^{-3} g.L^{-1}$ $K_X = 3.932 g.L^{-1}$

[a] $\boldsymbol{C}$ and $\boldsymbol{P}$ are concentration of carbon and phosphorus in the media respectively, and $\boldsymbol{\alpha_{Cmax}}$ and $\boldsymbol{\alpha_{Pmax}}$ are model constant regarding these values.
[b] $\boldsymbol{X}$ is the concentration of biomass, $\boldsymbol{L}$ is the concentration of lipid and $\boldsymbol{Q}$ is nitrogen concentration within the cell.
[c] $\boldsymbol{X_{max}}$ is the maximum sustainable concentration of biomass.

variations of nutrients concentration; however, this model has proven to be more successful in explaining microalgae growth compared to Monod equation.

Applying the above models many studies used concentration of nutrients in the culture and related it to the growth rate [36,39,106,107]; However, some believed that the concentration in the media does not have an immediate effect on the specific growth rate unless a long-term rate is studied [109,110]. Also, it has been reported that even when the concentration of nutrients in the culture dropped to zero, microalgal growth was not immediately ceased [109–111]. Martinez Sancho et al. [112] tried to resolve this issue with classical Monod model by introducing an extra parameter in the model. They examined different models for phosphorus-limited cultures, including a modified form of Monod equation which showed a better fit to the experimental results:

$$\mu = \frac{\mu_{m1}S + \mu_{m2}K_S}{K_S + S} \tag{15}$$

In this model μ_{m1} is maximum specific growth rate, and μ_{m2} is specific growth rate when there is no phosphorus. By adding the specific growth rate at zero phosphorus concentration they tried to explain the ongoing growth after consumption of all nutrients. Later, they examined other models for inhibitory effect of substrate where they modified Andrew's equation and formed a new model [113].

$$\mu = \frac{\mu_{m1}K_iS + \mu_{m2}S^2 + \mu_{m3}K_SK_i}{K_SK_i + K_iS + S^2} \tag{16}$$

Where μ_{m1} is maximum specific growth rate, μ_{m2} is inhibited growth rate, and μ_{m3} is the specific growth rate when there is no phosphorus. Also K_S and K_i are model constants to account for saturation and inhibition by substrate, respectively.

Another approach was presented by introducing the concept of intercellular concentration or cell quota where it is assumed that nutrients are stored within the cell before it is used. Droop [110,114,115] suggested that cell quota, which is customarily represented by Q and is defined as the concentration of nutrient within the cell divided by cell mass, could be used as an effective parameter to calculate the specific growth rate:

$$\mu = \mu'_{max}\left(1-\frac{k_Q}{Q}\right) \tag{17}$$

k_Q is the saturation constant which later was referred to by some researchers [2,116] as Q_{min} implying that if the cell quota of a specific nutrient is less than Q_{min} , the growth rate will be zero. Therefore, when the substrate concentration reaches zero in the culture, there is still nutrients stored in the cell to support cell growth. This model proved to be successful in describing the behaviour of microalgae in natural systems when nitrogen and phosphorus are both limited [2,117,118]. Droop's equation has become a well-known model and has been frequently used by many researchers [25,29,101,119] because it is able to uncouple the growth rate and the absorption of the nutrients [120]. Sommer [121] compared Monod and Droop models using data from a eutrophic lake in Germany and found Monod model to be significantly less accurate than Droop. He also explained while Monod model has limitation in its application due to luxury uptake of nutrients, Droop model is difficult to apply as cell quota is difficult to measure.

Caperon and Meyer [122,123] used the same concept as Droop and proposed another model using Michaelis-Menten form of equation:

$$\mu = \mu'_{max}\frac{Q - Q_{min}}{Q - Q_{min} + K_C} \tag{18}$$

Where K_C is the model constant.

This model was developed to explain steady state growth rate under nutrient-limited condition. Later, Flynn [111] used the same model as a basis to explain co-limitation of nitrogen and phosphorus. He assumed that at Q_{max} the specific growth rate is maximised which led to the following equation:

$$\mu = \mu'_{max}\frac{\frac{Q - Q_{min}}{Q - Q_{min} + K_C}}{\frac{Q_{max} - Q_{min}}{Q_{max} - Q_{min} + K_C}} \tag{19}$$

Another assumption was that K_C is a linear function of $Q_{max} - Q_{min}$ which ultimately resulted in Eq. (19):

$$\mu = \mu'_{max}\frac{(1+K_Q)(Q - Q_{min})}{(Q - Q_{min}) + K_Q(Q_{max} - Q_{min})} \tag{20}$$

where K_Q is the model constant.

Eq. (20) can be simplified to:

$$\mu = \mu'_{max}\frac{\hat{Q}(1+K_Q)}{\hat{Q} + K_Q} \tag{21}$$

$$\hat{Q} = \frac{Q - Q_{min}}{Q_{max} - Q_{min}} \tag{22}$$

In this model, if the quota reaches its maximum value, which is finite, the growth rate will be at its maximum as well, but this statement does not apply to Droop's model. In Droop's model in order to reach the maximum growth rate, the cell quota needs to approach infinity which is not a realistic assumption. However, Droop [124] explained that μ'_{max} is merely a mathematical concept which can only be achieved when Q approaches infinity and it is different from maximum specific growth rate in Monod equation (μ_{max}) and its value is larger than μ_{max} [125].

Table 3
Models considering the effect of temperature.

Source	Model		System	Alga type	Estimation
Ratkowsky et al. [142]	$\sqrt{\mu} = b(T-T_0)$	(1)		*For Bacteria*	
Ratkowsky et al. [143]	$\sqrt{\mu} = b(T-T_{min})(1-e^{c(T-T_{max})})$	(2)		*For Bacteria*	
Zwieterin et al. [147]	$\mu = b(T-T_{min})^2(1-e^{c(T-T_{max})})$	(3)		*For bacteria*	
James and Boriah [95]	$\mu = \mu_{max}\exp(-k_t(T-T_{opt})^2)$	(4)	Indoor	*Phaeodactylum tricornutum*	$T_{opt} = 20°C$ $k_t = 0.007°C^{-2}$
Franz et al. [72]			-	-	$T_{opt} = 25°C$ $s = \frac{1}{\sqrt{k_t}} = 13°C$
Jayaraman and Rhinehart [18]			-	*Gladieria sulphuraria*	$T_{opt} = 323K$ $k_t = 0.0001K^{-2}$
Dauta et al. [58]	$\mu = \begin{cases} \mu_{max}\exp\left(-2.3\left(\frac{T-T_{opt}}{T_L-T_{opt}}\right)^2\right), T<T_{opt} \\ \mu_{max}\exp\left(-2.3\left(\frac{T-T_{opt}}{T_U-T_{opt}}\right)^2\right), T\geq T_{opt} \end{cases}$	(5)	Indoor	*Chlorella Vulgaris*	$T_{opt} = 30°C$
				Fragilaria crotonensis	$T_{opt} = 25°C$
				Straurastrum pingue	$T_{opt} = 27°C$
				Synechocystis minima	$T_{opt} = 32°C$
Franz et al. [72]	$\frac{\mu}{\mu_{max}} = \begin{cases} \exp\left(-\left(\frac{T-T_{opt}}{s}\right)^2\right), T\leq T_{av,day} \\ 1, \quad T_{av,day}<T\leq T_{av,day}+8 \\ \exp\left(-\left(\frac{T-T_{opt}+8}{s}\right)^2\right), T>T_{av,day}+8 \end{cases}$	(6)	Outdoor	*Chlamydomonas reinhardtii*	• *Tromsø:* $T_{opt} = 7°C$ $s = 5°C$ • *Fehmarn:* $T_{opt} = 11°C$ $s = 5°C$ • *Karlsruhe* $T_{opt} = 13°C$ $s = 6°C$ • *Madrid* $T_{opt} = 17$ • *Tamanrasset* $T_{opt} = 25°C$ • *Manaus:* $T_{opt} = 28°C$ $s = 10°C$
James et al. [157]	$\frac{\mu}{\mu_{max}} = \begin{cases} \exp(-K_1(T-T_1)^2), T\leq T_1 \\ 1, \quad T_1<T\leq T_2 \\ \exp(-K_2(T-T_2)^2), T>T_2 \end{cases}$	(7)			
Costache [82]	$P = P_{max}(k_1 e^{E_1/RT} - k_2 e^{E_2/RT})$	(8)	Indoor	*Scendesmus almeriensis*	$k_1 = 4.99\times10^7$ $k_2 = 1.66\times10^{13}$ $E_1 = 4.27\times10^4 mol.J^{-1}$ $E_2 = 7.71\times10^4 mol.J^{-1}$
Bitaube Perez et al. [158]	$\mu = \mu_{max}\left(k_1\exp\left(\frac{E_1}{RT}\frac{T-T_0}{T_0}\right) - k_2\exp\left(\frac{E_2}{RT}\frac{T-T_0}{T_0}\right)\right)$	(9)	Indoor	*Phaeodactylum tricornutum*	$k_1 = 0.26h^{-1}$ $k_2 = 0.18h^{-1}$ $E_1 = 28kcal.\ mol^{-1}$ $E_2 = 39kcal.\ mol^{-1}$ $T_0 = 293K$
Tevatia et al. [159]	$\mu = \mu_{max}\left(\frac{e^{E_1/RT}}{1+K_T e^{E_2/RT}}\right)$	(10)		*Chlamydomonas reinhardtii*	
Sharpe and DeMichele [145]	$\mu = \frac{\frac{\phi}{TeR}-\frac{\Delta H_A}{RT}}{1+e^{\frac{\Delta S_L}{R}-\frac{\Delta H_L}{RT}}+e^{\frac{\Delta S_H}{R}-\frac{\Delta H_H}{RT}}}$	(11)		*Chlorella sorkiniana*	$\phi = 32.69(K^{-1}s^{-1})$ $\Delta H_A = 12939\left(\frac{cal}{mol}\right)$ $\Delta S_H = 180.2\left(\frac{cal}{mol.K}\right)$ $\Delta H_H = 56977\left(\frac{cal}{mol}\right)$ $\Delta S_L = -184.4\left(\frac{cal}{mol.K}\right)$ $\Delta H_L = -54632\left(\frac{cal}{mol}\right)$
Eppley [153]	$\mu = \mu_0 1.066^T$	(12)	indoor	Approximately 130 species	$\mu_0 = 0.851 doublings\ per\ day$
Moisan [160]	$\mu = \begin{cases} \log(2)*0.851*1.066^T e^{\frac{\lvert T-T_{opt}\rvert^3}{T_{low}}}, T\leq T_{opt} \\ \log(2)*0.851*1.066^T e^{\frac{\lvert T-T_{opt}\rvert^3}{T_{high}}}, T>T_{opt} \end{cases}$	(13)			
Norberg [161]	$\mu = 0.59\left(1-\left(\frac{T-Z}{w}\right)^2\right)e^{0.0633T}$	(14)			
Haario et al. [70]	$\mu = \mu_{ref}\theta^{T-20}$	(15)	outdoor	Diatom	$\mu_{ref} = 0.0886day^{-1}$ $\theta = 1.14$

(*continued on next page*)

Table 3 (*continued*)

Source	Model		System	Alga type	Estimation
				Chrysophycea	$\mu_{ref} = 0.0465 day^{-1}$ $\theta = 1.07$
				Cyanobacteria	$\mu_{ref} = 0.329 day^{-1}$ $\theta = 1.16$
				Minor species	$\mu_{ref} = 0.212 day^{-1}$ $\theta = 1.13$
Lee and Zhang [76]			Indoor	*Chlorella* sp.	When coupled with Chalker [48] model of light: $\theta = 1.35$ When coupled with Muller-Feuga [100] model of light: $\theta = 1.16$
Pegallapati and Nirmalakhandan [80]	$\mu = \mu_{ref} 1.066^{T-20}$	(16)	Indoor	*Nannochloropsis salina* *Scenedesmus* sp.	$\mu_{ref} = 1.2 day^{-1}$ $\mu_{ref} = 1.4 day^{-1}$
Ketheesan and Nirmalakhandan [154]			Indoor and outdoor	*Nannochloropsis salina*	Indoor: $\mu_{ref} = 2.0 day^{-1}$ Outdoor: $\mu_{ref} = 1.15 day^{-1}$
Sukenik et al. [30,156]	$P = P_{ref} \exp\left(-E_0\left(\frac{1}{T} - \frac{1}{T_{ref}}\right)\right)$	(17)	Indoor	*Dunaliella tertiolecta*	$E_0 = 3500$ K
Geider et al. [92]				*Pavlova lutheri* *Skeletonema costatum* *Thalassiosira pseudonana* *Isocrysis galbana*	
Chen et al. [130]	$\mu = \mu_{max} c_1 e^{c_2 \lvert T - T_{opt} \rvert}$	(18)		*Micrpcystis aeruginosa*	$c_1 = 1.57$ $c_2 = 0.24$
Carvalho and Malcata [99]	$\mu = \mu_{max}\left(1 - \frac{X}{X_{max}}\right)$ $\mu_{max} = \frac{K_1 I}{K_2 T + I} e^{-\frac{K_3 I}{RT}}$ $X_{max} = (K_4 + K_5 T) e^{-\frac{K_6 L}{RT}}$	(19)	indoor	*Pavlova lutheri*	$K_1 = -2.72 day^{-1}$ $K_2 = -2.86 °C^{-1}$ $K_3 = 129 \times 10^2 J.\ mol^{-1}$ $K_4 = 1.19 \times 10^8 cell.\ mL^{-1}$ $K_5 = -3.69 \times 10^5 cell.(mL.\ °C)^{-1}$ $K_6 = -12.4 J.\ mol^{-1}$
Bernard and Remond [15]	$\mu = \mu_{max} \frac{(T - T_{max})(T - T_{min})^2}{(T_{opt} - T_{min})(a(T) - b(T))}$ $a(T) = (T_{opt} - T_{min})(T - T_{opt})$ $b(T) = (T - T_{opt})(T_{opt} + T_{min} - 2T)$ $T_{min} < T < T_{max}$	(20)	Indoor	Various species	Parameters are available in [15]
Munoz-Tamayo [89]			Indoor		$\mu_{max} = 0.76 day^{-1}$ $T_{min} = -0.2$°C $T_{opt} = 26.7$°C $T_{max} = 33.3$°C
Ippoliti et al. [12]	$P = P_{max} \frac{(T - T_{max})(T - T_{min})^2}{(T_{opt} - T_{min})(a(T) - b(T))}$ $a(T) = (T_{opt} - T_{min})(T - T_{opt})$ $b(T) = (T - T_{opt})(T_{opt} + T_{min} - 2T)$ $T_{min} < T < T_{max}$	(21)	Indoor and outdoor	*Isochrysis galbana*	$T_{min} = 11.88$°C $T_{opt} = 35.73$°C $T_{max} = 46.15$°C
Rarrek et al. [162]	$f(T) = 1 - \lvert T - T_{opt} \rvert T_{dep}$	(22)			$T_{opt} = 25$°C $T_{dep} = 0.05 K^{-1}$
Blanchard et al. [152]	$P = P_{max} \phi_T^{\beta} e^{\beta(1-\phi_T)}$ $\phi_T = \frac{T_{max} - T}{T_{max} - T_{opt}}$	(23)	Indoor	*Benthic diatom*	Isolated in September 1995 $P_{max} = 5.81 \mu g\ C\ (\mu g\ Chl\ a)^{-1} h^{-1}$ $T_{opt} = 25.3$°C $T_{max} = 38.2$°C $\beta = 1.76$ Isolated in December 1995 $P_{max} = 3.04 \mu g\ C\ (\mu g\ Chl\ a)^{-1} h^{-1}$ $T_{opt} = 25.4$°C $T_{max} = 34.9$°C $\beta = 1.03$
Slegers et al. [163]			Indoor	*Phaeodactylum tricornutum*	$T_{opt} = 21.64$°C $T_{max} = 30.31$°C $\beta = 1.57$
				Thalassiosira pseuinana	$T_{opt} = 24.73$°C $T_{max} = 31.4$°C $\beta = 1.83$
Quinn et al. [116]	$\mu = \mu_{max} \frac{2k_T}{1 + k_T^2}$ $k_T = \exp\left(\frac{E_a}{RT_{opt}} - \frac{E_a}{RT}\right)$	(24)	Outdoor	Nannochloropsi oculta	$E_a = 63 kJ\ mol^{-1}$ $T_{opt} = 23$°C

Bougaran et al. [120] proposed a threshold coupling model that considered both phosphorus and nitrogen limitation where the minimum quota function is related to the specific growth rate. They proposed the same form of function for both N and P:

$$\mu = \mu'_{max} \frac{1-\frac{Q_{min}}{Q}}{1-\frac{Q_{min}}{Q_{max}}} \tag{23}$$

This equation resolves the infinite quota problem with Droop's model by adding a maximum quota as well as maintaining the simplicity of the equation.

Another model was proposed by Guest et al. [126] which used the same condition as Bougaran (threshold model for N and P) and Droop's model as a basis.

$$\mu = \mu'_{max}\left(1-\left(\frac{Q_{min}}{Q}\right)^4\right) \tag{24}$$

Even though this equation still has the same issue with infinite quota as Droop's model, due to the fourth power, the function rapidly reaches the vicinity of its maximum value where its difference from maximum is negligible for common values of Q. This makes the model appropriate when compared to the experimental data.

Another aspect of modelling the effect of nutrient, is understanding the relationship when there is more than one nutrient involved. Haefner [127] presented five methods for combining multiple parameters: (1) Liebig's law of minimum, (2) multiplication, (3) arithmetic average, (4) mean resistance, and (5) additive rates.

Liebig's law of minimum, which is also known as threshold model, assumes that the most limited nutrient determines the rate of growth. Therefore, it describes the growth to be related to minimum value of nutrients functions:

$$\mu = \mu_{max}\min(f(S_1), f(S_2), f(S_3)) \tag{25}$$

The function of each nutrient can be any of the discussed models such as Monod or Droop models.

Multiplication method assumes that all the nutrients affect the growth at the same time and not only limitation in one nutrient lowers the growth rate, but multiple limitations deteriorate the situation. It relates the final value to be relative to multiplication of all functions:

$$\mu = \mu_{max}.f(S_1).f(S_2).f(S_3) \tag{26}$$

The third method is using the arithmetic average of the functions:

$$\mu = \mu_{max}\frac{f(S_1)+f(S_2)+f(S_3)}{3} \tag{27}$$

Mean resistance method is inspired by the effect of a resistance in an electrical circuit and uses the reverse of each function:

$$\mu = \mu_{max}\frac{1}{\frac{1}{f(S_1)}+\frac{1}{f(S_2)}+\frac{1}{f(S_3)}} \tag{28}$$

Haefner [127] added the fifth method (additive rates) based on a study by O'Neill et al. [128] where they compared eight different methods of simultaneous limitation by applying them to data from terrestrial and aquatic experiments, and found additive model to be the most accurate.

$$\mu = \mu_{max}\frac{S_1S_2}{K_1S_2+S_1S_2+K_2S_1} \tag{29}$$

As can be seen, this equation is based on the Monod model.

Among all the mentioned methods, two approaches are the most common among the researchers when modelling co-limitation of nutrients: threshold model and multiplicative model [2]. Multiplicative model, unlike threshold model, has been used widely and not only for co-limitation, but also for connecting the effects of other parameters such as light and temperature; however, Haefner [127] stated that in practice using multiplication appears to underestimate growth when the number of limiting nutrients increase.

Law of the minimum was employed in the model proposed by Bougaran et al. [120] and Guest et al. [126]. As in the latter study, the co-limited relationship was expressed with the following equation:

$$\mu = \mu_{max}\min\left(\left(1-\left(\frac{Q_{P,min}}{Q_P}\right)^4\right),\left(1-\left(\frac{Q_{N,min}}{Q_N}\right)^4\right)\right) \tag{30}$$

2.3. Temperature

After nutrient and light, temperature plays the most crucial role in the growth of microalgae [15]. Many studies have been undertaken to understand the effect of temperature on the growth rate and many models have been proposed in a variety of forms (Table 3). This diversity in the form of models suggests the complicated nature of the relationship between growth and temperature.

Many of the models for effect of temperature on the growth of microalgae are inspired from bacterial or other microbial growth models. Hence, all seem to follow similar trends.

One of the first models is known as Hinshelwood model [141] which was derived using Arrhenius law for growth of bacteria and later was used for microalgae growth:

$$\mu = k_1e^{-\frac{E_1}{T}} - k_2e^{-\frac{E_2}{T}} \tag{31}$$

where T is absolute temperature and k_1, k_2, E_1, and E_2 are model parameters. E_1 and E_2 replaced the activation energy over gas constant ($\frac{E_a}{R}$) in the original form of Arrhenius law and k_1 and k_2 are pre-exponential factors. Thermodynamically, in this equation, the first term can be interpreted as the production (growth) rate and the second term as the consumption (death) rate of the bacteria due to high temperature. However, as the temperature is decreased in this model, specific growth rate declines but never reaches zero except at temperature of absolute zero. This makes the model unrealistic at low temperatures.

Ratkowsky et al. [142] explain that Van't Hoff and Arrhenius relations cannot provide a good approximation of the temperature dependency of the growth rate. They plotted the logarithm of the growth rate against the reciprocal of absolute temperature and suggested the following model which uses the square root of growth rate:

$$\sqrt{\mu} = b(T - T_{min}) \tag{32}$$

where T_{min} is the temperature below which no growth takes place and b is the model constant.

However, this equation worked well from the minimum temperature to the optimum temperature, where the growth rate is at its maximum value, but for higher temperatures this equation is not valid. When the temperature is increased beyond the optimum value, the growth rate starts to decrease while this equation does not predict this effect. To cover this flaw, an extension of this model was proposed [143]. In the new model an exponential term was added to correct the previous equation for higher temperatures:

$$\sqrt{\mu} = b(T - T_{min})(1-e^{c(T-T_{max})}) \tag{33}$$

where T_{max} is the maximum temperature limit for growth and c is a model constant. They applied this model to 30 sets of data for various bacteria and found this model to be fairly accurate.

Sharpe et al. [144,145] proposed a model considering three energy states: (1) inactivation due to low temperature, (2) inactivation due to high temperature, and (3) active (developing) state. They modelled the transition between the states and used a different equation for the kinetic rates to describe the growth rate changes with temperature:

$$\mu = \frac{T\exp\left(\frac{\left(\phi - \frac{\Delta H_A}{T}\right)}{R}\right)}{1+\exp\left(\frac{\left(\Delta S_L - \frac{\Delta H_L}{T}\right)}{R}\right) + \exp\left(\frac{\left(\Delta S_H - \frac{\Delta H_H}{T}\right)}{R}\right)} \quad (34)$$

In this equation R is the universal gas constant, and the rest of the parameters are defined as follows:

- ΔH_A: enthalpy of activation of growth
- ΔS_L: entropy change of low temperature inactivation
- ΔH_L: enthalpy change of low temperature inactivation
- ΔS_H: entropy change of high temperature inactivation
- ΔH_H: enthalpy change of high temperature inactivation
- ϕ: is the model constant

Schoolfield et al. [146] described this formulation to be unsuitable for regression due to high correlation of parameters. They explained that the complexity of the model makes parameter estimation sometimes impossible. Therefore, they reformulated the function to facilitate the regression process.

$$\mu = \frac{\mu_{25}\frac{T}{298}\exp\left(\frac{\Delta H_A}{R}\left(\frac{1}{298} - \frac{1}{T}\right)\right)}{1+\exp\left(\frac{\Delta H_L}{R}\left(\frac{1}{T_L} - \frac{1}{T}\right)\right) + \exp\left(\frac{\Delta H_H}{R}\left(\frac{1}{T_H} - \frac{1}{T}\right)\right)} \quad (35)$$

Schoolfield et al. [146] used 25 °C (298 K) as the reference temperature and included specific growth rate at this temperature (μ_{25}) as one of the parameters in the model. The reason for selection of 25 °C as the reference temperature was mainly due to observed high activity for most microalgae around this temperature. In Eq. (34) T_L and T_H are temperatures of half-inactivation at low and high temperature, respectively.

Zwietering et al. [147] modified the extended Ratkowsky model, so that the growth rate is related to the square of the first term but not the exponential term.

$$\mu = (b(T - T_{min}))^2(1-e^{c(T-T_{max})}) \quad (36)$$

Then, they compared the modified model with several other models including Schoolfield [146] and Ratkowsky [142,143] models for growth of enzymes and reported that despite having only four parameters, their model had less deviation from experimental data than more complicated models like Schoolfield's. Lobry et al [148] suggested a new empirical model using three cardinal temperatures (T_{min}, T_{opt} and T_{max}). The growth takes place when the temperature is between T_{min} and T_{max}, therefore, out of this range there is no positive growth and at T_{opt} the specific growth rate reaches its maximum value. These three temperatures are part of the characteristics of each species and having a model based on these values facilitates the application of the model.

$$\mu = \mu_{max}\frac{(T_{max} - T)(T - T_{min})}{(T - T_{opt})^2 + (T_{max} - T)(T - T_{min})} \quad (37)$$

This model was unable to predict the suboptimal curve of growth with temperature, thus it was modified and cardinal temperature model with inflection (CTMI) was introduced [141]:

$$\mu = \mu_{max}\frac{(T - T_{max})(T - T_{min})^2}{(T_{opt} - T_{min})[(T_{opt} - T_{min})(T - T_{opt}) - (T_{opt} - T_{max})(T_{opt} + T_{min} - 2T)]} \quad (38)$$

Rosso et al. [141] compared the new model with Ratkowsky [143] and Zwietering [147] model for 47 sets of data of various bacterial species. The comparison showed that CTMI was able to show a better fit for 21 of the 47 sets while Ratkowsky model performed better for 20 of the 47 sets and in the remaining six sets Zwietering model had the lowest deviation. The performance of this model was very close to that of Ratkowsky model, but its ease of use and meaningful parameters made CTMI a powerful tool which later was used by Bernard et al. for microalgal cultures [15]. They used CTMI for various algal species and showed its good fit with experimental data. However, it must be mentioned that CTMI has certain limitations in terms of its applicability. To have positive values for μ all across the valid range, the average of T_{min} and T_{max} should be less than T_{opt} or in other words T_{opt} needs to be closer to T_{max} than T_{min} , otherwise the model will produce negative numbers for growth [15].

In 1999 Yan and Hunt [149] used cardinal temperatures to predict the change in photosynthetic rate of plants by temperature, modifying previous models by Yin et al. [150] and Gao et al. [151] for growth in crops.

$$\mu = \mu_{max}\frac{T_{max} - T}{T_{max} - T_{opt}}\left(\frac{T - T_{min}}{T_{opt} - T_{min}}\right)^{\frac{T_{opt} - T_{min}}{T_{max} - T_{opt}}} \quad (39)$$

The model, then was further simplified by assuming T_{min} to be zero which led to the following equation:

$$\mu = \mu_{max}\frac{T_{max} - T}{T_{max} - T_{opt}}\left(\frac{T}{T_{opt}}\right)^{\frac{T_{opt}}{T_{max} - T_{opt}}} \quad (40)$$

Another model was proposed by Blanchard et al. [152] for the change in growth of motile benthic diatoms with temperature. Although, the model seems to fit the experimental data acceptably, it is observed that in suboptimal temperatures the model predicted a smaller degree of curvature compared to that of experiments.

Some studies used a normal distribution model (Gaussian curve) to predict the effect of temperature [18,95]. In this model, growth is maximum around T_{opt} and as the temperature decreases or increases the growth will change in a Gaussian bell-shape. In a study, Franz et al. [72] used Gaussian curve to explain the effect of temperature and assumed that microalgal strains had adapted to local climate, and therefore, had the best performance at average temperature of their specific geographical location. They suggested two equations: the first one assumes T_{opt} to be average temperature for all the studied locations:

$$\mu = \mu_{max}\exp\left(-\left(\frac{T - T_{opt}}{s}\right)^2\right) \quad (41)$$

and the second equation takes $T_{ave,day}$ equal to the average temperature of each location:

$$\left\{\mu = \mu_{max}\exp\left(-\left(\frac{T - T_{ave,day}}{s}\right)^2\right); T \le T_{ave,day}\right. \quad (42)$$

$$\{\mu = \mu_{max}; T_{ave,day} < T \le T_{ave,day}+8 \quad (43)$$

$$\left\{\mu = \mu_{max}\exp\left(-\left(\frac{T - T_{ave,day}+8}{s}\right)^2\right); T_{ave,day}+8<T\right. \quad (44)$$

where s is a model constant.

As it can be seen, in the second model the growth rate stays at the maximum value for a temperature range of 8 °C which is due to the hypothesis that temperature has less effect on the growth rate when the light intensity is low [72] and ultimately makes the model application very limited. Moreover, the change in growth with temperature does not fully fit a Gaussian distribution as based on experimental data the change is not symmetrical. Dauta et al. [58] have also used the same basis for their model but added skewness to the functions to get the asymmetry in the shape of the model.

Eppley [153] proposed a very simple model for growth of various species of phytoplankton in the sea using about 200 data points.

$$\mu = 0.851 \times 1.066^{T} \quad (45)$$

Here T is temperature in degrees Celcius. This model is surprisingly simple and easy to use and many other researchers utilised it as a basis for their models [70,76,80,154]. However, this model only performs as an envelope for various species or in other words as the author stated the equation is "useful as a generalisation of the maximum μ to be expected for a photosynthetic unicellular algae." [153]

So far in all the discussed models the effect of temperature was as an independent and separate function which could be coupled with that of other limiting factors. But there are studies that included the effect of temperature in other functions such as light [155]. For instance, Dermoun et al. [87] (Eq. (14) in Table 1) and Talbot et al. [86] (Eq. (13) in Table 1) used the Peeters and Eilers model [54,56] for light but considered the constants to be temperature dependant. Grobbelaar [88] used the same principle but applied it to Baly's model [36].

$$\mu = a_1 a_2^{\theta} \frac{K_S a_3^{\theta} I}{I + K_S a_3^{\theta}} \quad (46)$$

In this equation a_1, a_2, and a_3 are model constants, K_S is light saturation constant, and θ is temperature factor calculated via following equation:

$$\theta = \frac{T-10}{10} \quad (47)$$

where T is temperature in ˚C.

As it can be seen, the effect of temperature on the growth of microalgae can be difficult to model and having numerous equations in variety of forms is a proof for it. Most of the studies reviewed here used a standalone function to describe this effect with a few cases where it was combined with light function. There are also studies where photosynthesis was described as a function of temperature and was later used to calculate specific growth rate or productivity assuming they have a linear relationships [30,91,92,156]:

$$P = P_{ref} \exp\left(-E_0\left(\frac{1}{T} - \frac{1}{T_{ref}}\right)\right) \quad (48)$$

where P_{ref} is photosynthesis rate at T_{ref}. Eq. (48) was inspired by Van 't Hoff equation which was originally derived to describe variation of equilibrium constant with temperature in a chemical reaction.

2.4. pH and carbon

For each strain of microalgae, there is an optimum pH where the growth rate is maximised [164]. But pH is a parameter which is closely affected by the amount of carbon in the media, as carbon dioxide injection is a common way to lower pH level [165]. In modelling approaches, their effects are considered together, thus only one of them is included in the models. Moreover, carbon is one of the main nutrients for algal growth and in many studies the same models used for nutrients, was applied to carbon as well [80,104,129]. However in the studies considering the effect of pH, the models were diverse. Also, in some studies pH was maintained constant using other means while carbon dioxide concentration was varied [17]. Table 4 summarises the models considering the effect of pH or carbon on the growth of microalgae.

Dissolved inorganic carbon in a culture can be in different forms such as carbon dioxide, carbonate, and bicarbonate [166] and they do not contribute equally to the growth. Algal cells use carbon dioxide to a larger extent compared to bicarbonate and barely use carbonate [167]. For pH levels between 6.5 and 10, where most of algal cells grow, bicarbonates are the dominant form of carbon (Fig. 2).

As mentioned before models that include the effect of carbon concentration treat carbon as a nutrient. Goldman et al. [104] used Monod model (Eq. (8) in Table 4) to relate specific growth rate to total inorganic carbon for *Scenedesmus quadricauda* and *Selenastrum capricornutum*. To calculate total inorganic carbon they added the amount of carbonic acid, bicarbonate and carbonate, as well as aqueous carbon dioxide. They stated that algal growth should be related to total inorganic carbon not one specific form of it. However, King and Novak [168] used the data from Goldman et al. [104] and argued that specific growth rate is a function of free carbon dioxide and not total inorganic carbon. Lee and Zhang [76] also used aqueous carbon dioxide in Monod model (Eq. (8) in Table 4) for growth of *Chlorella* sp. when concentration of carbon dioxide is below 50 mg L^{-1}. For higher concentrations Andrews model was utilised to include the inhibitory effect of carbon caused by low pH as a result of high carbon concentration. Baquerisse et al. [94] selected Steele model [52], which was originally used for irradiance, and replaced light parameters with carbon dioxide parameters to explain the growth kinetic of *Porphyridium purpureum*.

The second type of models are those where pH level is incorporated directly into the model. Bailey and Ollis [169] derived a model for the effect of pH on the reaction rate of enzymes:

$$\mu = \mu_{max} \frac{1}{1 + \frac{[H^+]}{K_H} + \frac{K_{OH}}{[H^+]}} \quad (49)$$

In this equation K_H and K_{OH} are model parameters and $[H^+]$ is hydrogen ion concentration which can be calculated from pH ($[H^+] = 10^{-pH}$). They classified enzymes into three groups: (1) catalytically active, (2) acid inactive, and (3) basic inactive. The same formulation was used by Tang et al. [170] for bacterium *Clostridium formicoaceticum* and later by Bitaube Perez et al. [158] for *Phaeodactylum tricornutum*. Zhang et al. [132] modified this model by adding a third constant to denominator and resulting in Eq. (50):

$$\mu = \mu_{max} \frac{1}{K_1 + \frac{[H^+]}{K_H} + \frac{K_{OH}}{[H^+]}} \quad (50)$$

where K_H, K_{OH} and K_1 are model parameters Jayaraman and Rhinehart [18] included pH as a parameter in their model assuming only carbon dioxide concentration is responsible for pH changes. Therefore, instead of using carbon dioxide concentration as an input, they used a function of pH to describe the effect of carbon.

$$\mu = \mu_{max} \cdot \frac{1}{1 + e^{\lambda(pH - pH_{opt})}} \quad (51)$$

Where pH_{opt} is the pH at which growth is maximised and λ is the model constant.

Costache et al. [82] used a model based on Arrhenius equation to describe the effect of pH on Photosynthesis rate which showed a close fit to experimental data for *Scendesmus almeriensis*:

$$P = P_{max}\left(B_1 e^{-C_1/pH} - B_2 e^{C_2/pH}\right) \quad (52)$$

In this equation B_1, B_2, C_1, and C_2 are model constants and P and P_{max} are photosynthesis rate and its maximum value respectively. Filali et al. [71], however, considered all three types of inorganic carbon (CO_2, HCO_3^-, and CO_3^{2-}) and by using equilibrium constants and pH, calculated the total amount of inorganic carbon.

$$\mu = \mu_{max} \cdot \frac{[TIC]}{X.\ K_{CL} + [TIC]} \quad (53)$$

$$[CO_2] = \frac{[TIC]}{1 + \frac{K_1}{[H^+]} + \frac{K_1 K_2}{[H^+]^2}} \quad (54)$$

$$[H^+] = 10^{-pH} \quad (55)$$

$$CO_2 + H_2O \leftrightarrow HCO_3^- + H^+ \quad (56)$$

$$HCO_3^- \leftrightarrow CO_3^{2-} + H^+ \quad (57)$$

Where $[TIC]$ is the molar concentration of total inorganic carbon, K_1 and K_2 are equilibrium constants of HCO_3^- and CO_3^{2-} formation (Eqs. (55) and (56)), X is biomass concentration, and K_{CL} is carbon saturation

Table 4
Models considering the effect of pH or carbon concentration.

Source	Formula		System	Alga type	Estimation
Jayaraman and Rhinehart [18]	$\mu = \mu_{max}\frac{1}{1+\exp(\lambda(pH-pH_{opt}))}$	(1)		*Gladieria sulphuraria*	$pH_{opt} = 2.5$
Costache [82]	$P = P_{max}(B_1 e^{-C_1/pH} - B_2 e^{C_2/pH})$	(2)	Indoor	*Scendesmus almeriensis*	$B_1 = 2.5$ $B_2 = 533$ $C_1 = 6.45$ $C_2 = 69.2$
Fernandez et al. [83]			Outdoor	*Scendesmus almeriensis*	$B_1 = 2.4098$ $B_2 = 533.01$ $C_1 = 6.2684$ $C_2 = 68.8062$
Bailey and Ollis [169] **Tang et al.** [170]	$\mu = \mu_{max}\frac{1}{1+\frac{[H^+]}{K_H}+\frac{K_{OH}}{[H^+]}}$	(3)			
Bitaube Perez et al. [158]			Indoor	*Phaeodactylum tricornutum*	$\mu_{max} = 0.064h^{-1}$ $K_H = 2.3\times10^{-6}mol.L^{-1}$ $K_{OH} = 1.2\times10^{-10}mol.L^{-1}$
Zhang et al. [132]	$\mu = \mu_{max}\frac{1}{K_1+\frac{[H^+]}{K_H}+\frac{K_{OH}}{[H^+]}}$	(4)	Indoor	*Chlamydomonas reinhardtii*	For nitrate: $\mu_{max} = 1.4528h^{-1}$ $K_1 = 0.7602$ $K_H = 0.401\times10^{7}mol.L^{-1}$ $K_{OH} = 0.865\times10^{7}mol.L^{-1}$ For ammonium nitrate: $\mu_{max} = 1.2942h^{-1}$ $K_1 = 1.1835$ $K_H = 0.2826\times10^{7}mol.L^{-1}$ $K_{OH} = 0.666\times10^{7}mol.L^{-1}$ For urea: $\mu_{max} = 1.4198h^{-1}$ $K_1 = 0.3499$ $K_H = 0.2609\times10^{7}mol.L^{-1}$ $K_{OH} = 0.8042\times10^{7}mol.L^{-1}$
Rarrek et al. [162]	$\mu = \mu_{max}(1-\lvert pH-pH_{opt}\rvert pH_{dep})$ pH_{dep}: model parameter pH_{opt}: pH associated with maimum growth	(5)			$ph_{opt} = 8.5$ $pH_{dep} = 0.3$
Ifrim et al. [171]	$\mu = \mu_{max}x_{pH}e^{1-x_{pH}}$ $x_{pH} = \frac{pH-pH_{max}}{pH_{min}-pH}$ pH_{min}: minimum pH for growth pH_{max}: maximum pH for growth	(6)			
Ippoliti et al. [12]	$P = P_{max}\cdot\frac{(pH-pH_{max})(pH-pH_{min})^2}{(pH_{opt}-pH_{min})(a(pH)-b(pH))}$ $a(pH) = (pH_{opt}-pH_{min})(pH-pH_{opt})$ $b(pH) = (pH_{opt}-pH_{max})(pH_{opt}+pH_{min}-2pH)$ pH_{min}: minimum pH for growth pH_{max}: maximum pH for growth pH_{opt}: pH associated with maimum growth	(7)	Indoor and outdoor	*Isochrysis galbana*	$pH_{opt} = 7.34$ $pH_{min} = 2.24$ $pH_{max} = 10$
Monod model [38]	$\mu = \mu_{max}\frac{C}{K_S+C}$	(8)			
Goldman et al. [104]			Indoor	*Scenedesmus quadricauda*	$\mu = 2.29day^{-1}$ pH 7.1–7.21 $K_S = 0.3mg.L^{-1}$ pH 7.25–7.39 $K_S = 0.36mg.L^{-1}$ pH 7.44–7.61 $K_S = 0.71mg.L^{-1}$
			Indoor	*Selenastrum capricornutum*	$\mu = 2.45day^{-1}$ pH 7.05–7.23 $K_S = 0.4mg.L^{-1}$ pH 7.25–7.39 $K_S = 1.0mg.L^{-1}$ pH 7.43–7.59 $K_S = 1.2mg.L^{-1}$
Hsueh et al. [105]			Indoor	*Nannochloropsis* sp.	$K_S = 1.9mM$ $\mu_{max} = 3.5day^{-1}$
Marsullo et al. [96]			Indoor	*Phaeodactylum tricornutum* *Thalassiosira pseuinana*	C: $K_S = 0.001mol.m^{-3}$ C: $K_S = 0.001mol.m^{-3}$
Lee and Zhang [76]				*Chlorella* sp.	$N{:}K_S = 3.6mgL^{-1}$

(*continued on next page*)

Table 4 (*continued*)

Source	Formula		System	Alga type	Estimation
Filali et al. [71]	$\mu = \mu_{max}\frac{[TIC]}{X.K_{CL}+[TIC]}$ X: biomass concentration K_{CL}: model parameter	(9)	Indoor	*Chlorella vulgaris*	$\mu_{max} = 0.08h^{-1}$ $K_S = 1.28\times10^{-5}mol.10^{9}cell^{-1}$
De La Hoz Siegler et al. [136,137]	$\mu = \mu_{max}\frac{C}{K_S+C+\frac{C^2}{Ki}}$	(10)	Indoor	*Auxenochlorella protothecoides (Heterotroph)*	$\mu_{max} = 11.12day^{-1}$ $K_S = 15.03gL^{-1}$ $K_i = 47.4gL^{-1}$
Pegallapati and Nirmalakhandan [80]			Indoor	*Nannochloropsis salina*	$\mu_{max} = 1.2(day^{-1})$ $K_S = 2.316\times10^{-6}M$ $K_i = 0.0046M$
				Scenedesmus sp.	$\mu_{max} = 1.4(day^{-1})$ $K_S = 9.818\times10^{-4}M$ $K_i = 1M$
Abdollahi et al. [138]			Indoor	*Auxenochlorella protothecoides*	$\mu_{max} = 14.18day^{-1}$ $K_S = 8.45gL^{-1}$ $K_i = 49.5gL^{-1}$
Lee and Zhang [76]				*Chlorella* sp.	$K_S = 4.26mgL^{-1}$ $K_{iS} = 250mgL^{-1}$
Kasiri et al. [75]	$\mu = \mu_{max}\frac{C-C_0}{K_S+(C-C_0)+\frac{C^2}{Ki}}$ C_0: minimum concentration of carbon for growth	(11)	Indoor	*Chlorella kessleri*	$\mu_{max} = 0.73day^{-1}$ $K_S = 3.75mgL^{-1}$ $K_i = 1.79\times10^{3}mgL^{-1}$
Baquerisse et al. [94]	$\mu = \mu_{max}.\frac{C}{C_{opt}}e^{1-\frac{C}{C_{opt}}}$ C_{opt}: carbon concentration associated with maximum growth	(12)	Indoor	*Porphyridim purpureum*	

constant. They used mass transfer equations to calculate the amount of carbon dioxide in the culture and using the above equations determined total inorganic carbon concentration and specific growth rate.

$$[CO_2^*] = \frac{p_{CO_2}}{H_{CO_2}} \tag{58}$$

$$\frac{dTIC}{dt} = k_L a([CO_2^*] - [CO_2]) \tag{59}$$

p_{CO_2} is partial pressure of carbon dioxide in the air, H_{CO_2} is Henry's constant for solubility of carbon dioxide in the medium, $[CO_2^*]$ is the maximum obtainable concentration of carbon dioxide in the medium, and $k_L a$ is the mass transfer coefficient.

Ifrim et al. [171] presented an equation in which they used minimum and maximum pH thresholds for growth:

$$\mu = \mu_{max}\frac{pH - pH_{max}}{pH_{min} - pH}e^{1-\frac{pH-pH_{max}}{pH_{min}-pH}} \tag{60}$$

Ippoliti et al. [12] proposed an equation (Eq. (7) in Table 4) based on CTMI (originally developed to describe the effect of temperature on growth). They used pH thresholds as well as optimum pH for growth, which showed to be a good fit to the experimental data.

In most studies carbon dioxide is assumed to be in excess, and therefore its effect is neglected while in large-scale cultivation, the limitation of carbon is a common issue in microalgal cultures [166] particularly at high culture densities or when there is no carbon dioxide injection into the system and increasing the amount of carbon dioxide significantly improves the productivity [164]. Despite this, there are very few researchers who included CO_2 in their model as a limiting factor and mostly the same approach as other nutrients has been employed.

2.5. Salinity

microalgae production is a process that requires massive amount of water, and procuring it is a major challenge. Yang et al. [172] reported that to produce one kilogram of biodiesel, 3726 kg of water is needed. The cost of using fresh water significantly affects the viability of microalgae production. Considering the majority of areas where microalgae can have highest productivity have limited or no access to freshwater [7], use of saline water, in the form of seawater or underground saline water, is an inevitable option to grow microalgae in large scale [7]. However, there is another challenge when any type of saline water is used. Areas with high intensity of sunlight are the best locations for cultivating microalgae as a higher level of irradiance accelerates the growth rate. On the other hand, higher light intensity means more evaporation, especially for open ponds, which causes an increase in salinity level [173]. Some types of microalgae are compatible with high-salinity water: (1) marine, (2) halotolerant, and (3) halophilic microalgae [174]. Salinity is an important parameter for the growth of these microalgae [175], and different types of microalgae have different reactions to high salinity [175,176]. Some strains of marine microalgae such as *Tetraselmis* sp. show higher productivities compared to freshwater microalgae [177,178]. Fábregas et al. [179] observed the maximum cell density for *Tetraselmis suecica* in the range of 2.5–3.5% salinity, and below this range, the density dropped in proportion to salinity. Laing and Utting [180] found this range to be 2.5–3% for *Tetraselmis suecica* and 1.5–2.5% for *Isochrysis galbana*. Controlling the salinity of the culture is a difficult task, especially when one of the goals is to minimise the consumption of freshwater and also maximise nutrients utilisation. Fon Sing [181] discussed the importance of recycling the media to use the unconsumed nutrients which will eventually reduce the cost of production. However, using this strategy means a constant increase in the salinity of the media which can significantly affect photosynthesis and consequently growth rate [182]. But despite incredible advancements in understanding the physiology of salinity effects [183], its relationship with growth is still not clear [182]. Salinity can affect microalgae in three ways: (a) causing osmotic stress, (b) uptake or loss of ions which results in ion stress, and (c) causing changes in cellular ionic ratios [183]. None of those has been a subject of mathematical modelling. Any change in osmotic pressure leads to inhibition of photosynthesis or can cause swelling which may result in the cells being burst [184]. The effect of salinity becomes more critical considering that elevated salinity level in the culture puts the cells

under stress [185]. The stressed cells grow slower and start accumulating lipids [186,187] which is not a desirable behaviour in growth phase when cell number growth is the goal. If saline water is to be used for microalgae cultivation, it is vital to understand the effect of salinity on growth and how changes in salinity, whether it is gradual (due to evaporation) or sudden (due to the addition of recycled medium), affects the growth. But despite the importance of this process parameter, to the extent of authors' knowledge, no effort has been made to include this effect in mathematical models.

2.6. Oxygen

Oxygen build-up in the culture is a major issue in microalgal growth [188–190] as oxygen is a by-product of photosynthesis [191] and its concentration can reach over four times of air saturation in the culture [192] which constrains photosynthesis rate. This can happen in both closed photo bioreactors and open ponds; however, due to diffusion to atmosphere and use of paddle wheels, high concentration of dissolved oxygen is less prominent in open ponds [188]. This effect was first discovered by Warburg in 1920, who observed that photosynthesis of *Chlorella* was dropped significantly when culture was exposed to pure oxygen [193]. Inhibition of growth by elevated oxygen, mostly referred to as Warburg effect, has been observed in many plants as well [194]. Many researchers have reported a decrease in productivity when a high concentration of oxygen was present in algal cultures [188,192,195]. Ugwu et al. [191] demonstrated a decrease in the productivity when dissolved oxygen was increased from 120% of air saturation to 300%. When the culture was stripped of oxygen, photosynthesis rate of *C. vulgaris* was increased and when the medium was exposed to pure oxygen, the photosynthesis rate dropped by 35% [189]. Turner et al. [193] showed that when *Chlorella pyrenoidosa* was exposed to less than 20% oxygen concentration in gas phase, no significant increase in the photosynthesis was observed but when oxygen level exceeded 20%, inhibition up to 42% was recorded. Also in a test for *Chlorella vulgaris*, they observed that when the culture was exposed to air again, the level of inhibition decreased; however, they could not conclude if this is always reversible. Merrett and Armitage [196] found that decreasing oxygen level in air from 21% to 2% result in an increase in cell number for *Euglena gracilis* but when the same experiment was done for *Chlamydomonas reinhardtii* no such effect was observed. Torzillo et al. [197] believe that high oxygen concentration causes sensitivity to photoinhibition and therefore lowers productivity while lowering the temperature can deteriorate the situation and increase the sensitivity. Richmond [188] reported that in extremely high concentration of oxygen photooxidative death can happen. Although the limiting effect of accumulated oxygen on the photosynthesis and growth is well accepted and attempts have been made to predict the concentration of oxygen in the microalgal culture [189], very few models can be found to describe this effect [82,198] (Table 5). Miyachi et al. [199] proposed a second order equation for degree of inhibition:

$$H = 1-\frac{P}{P_{max}} = \frac{[O_2]^2}{K_O^2 + [O_2]^2} \tag{61}$$

where H is degree of inhibition, K_o is model constant, P is photosynthesis rate and P_{max} is photosynthesis rate at the absence of oxygen (replaced by nitrogen) and $[O_2]$ is oxygen partial pressure in gas phase. Fernandez et al. [81], however, used a first order Eq. (61) which resulted in Eq. (62).

$$P = P_{max}\frac{K_O}{K_O + [O_2]} \tag{62}$$

In a study to simulate a biocoil Photobioreactor, Concas et al. [3] used a linear function to describe the inhibitory effect of oxygen:

$$\mu = \mu_{max}\left(1-\frac{[O_2]}{[O_2]_{max}}\right) \tag{63}$$

In this equation $[O_2]_{max}$ is oxygen concentration at which growth becomes zero. Costache et al. [82] related photosynthesis rate to the rate of oxygen generation and developed the following equation:

$$P = P_{max}\left(1-\left(\frac{[O_2]}{K_{O_2}}\right)^z\right) \tag{64}$$

where K_{O_2} and z are the model constants.

3. Gaps and pathways for future researches

Despite the extensive and detailed studies in the modelling of the growth rate of microalgae, there is still room for improvement. Some of the gaps have been reported in previous reviews [2,51]; however there are still a number of areas which have not been addressed. The following areas are the most important areas of research to achieve better models for application in industrial systems:

3.1. Light

Light is one of the most important parameters in modelling the microalgae growth, and almost all suggested models have included the effect of this parameter and are thoroughly reviewed by Bechet et al. [51] and Lee et al. [2]. This does not mean that no more study can be done in this area. Contrarily, there are still a few ambiguities when it comes to irradiance. Firstly, how the light intensity should be utilised is

Table 5
Models considering the effect of dissolved oxygen.

Source	Formula		System	Alga	Estimation
Miyachi et al. [199]	$P = P_{max}\frac{K_O^2}{K_O^2+[O_2]^2}$	(1)			
Turner and Brittain [200]			Indoor	*Chlorella*	at $CO_2 = 1\times10^{-6}$ mol L^{-1} $K_O = 0.42$ atm at $CO_2 = 91\times10^{-6}$mol L^{-1} $K_O = 1.71$ atm
Costache et al. [82]	$P = P_{max}\left(1-\left(\frac{[O_2]}{K_O}\right)^z\right)$	(2)	Indoor	*Scendesmus almeriensis*	$K_O = 32.08$ mg L^{-1} $z = 5.49$
Fernandez et al. [83]			Outdoor	*Scendesmus almeriensis*	$K_O = 0.8373$ mol m^{-3} $z = 5.4333$
Ippoliti et al. [12]			Indoor and outdoor	*Isochrysis galbana*	$K_O = 19.99$ mg L^{-1} $z = 2.9$
Concas et al. [79]	$\mu = \mu_{max}\left(1-\frac{[O_2]}{[O_2]max}\right)$	(3)	Indoor	Spirulina platensis	$\mu_{max} = 2.06\times10^{-5}$ s^{-1} $[O_2]_{max} = 47.9$g m^{-3}
Fernandez et al. [81]	$P = P_{max}\frac{K_O}{K_O+[O_2]}$	(4)	Outdoor light	*Scendesmus almeriensis*	$K_O = 1.13$ mol O_2 m^{-3}

still a subject of debate, whether incident irradiance is more proper or average irradiance [2]. Some studies use incident [29,34,72] while some use average light intensity [71,154] and a few cases use both at the same time [59]. It must be well understood that which irradiance needs to be used and where it should be used to have the best outcome.

Additionally, it is widely known that just a particular spectrum of light (PAR) is influential on photosynthesis, and some wavelengths are absorbed better than the others. Considering that wavelengths have different penetration depth and therefore different distribution throughout the culture, it is clear that light spectrum and wavelength has a role to play in the growth models which is neglected in all the models. The only models where wavelengths played a role in light distribution in the culture was by Blanken et al. [27]. Therefore, more studies need to be done to formulate the effect of wavelength, as in the existing models, it is assumed that all wavelengths have the same effect on the growth rate.

The light application form is another debatable subject. As discussed by Bechet et al. [51], it is usually used in form of photon flux density (PFD), conventionally reported in $\mu E\ m^{-2}\ s^{-1}$ or $\mu mol\ photon\ m^{-2}\ s^{-1}$, or energy flux ($W\ m^{-2}$). Despite the popularity of the former, the latter is more convenient in energy studies. Using PFD is more justifiable considering the efficiency of photons with different wavelengths (as mentioned before), and energy flux is more applicable when looking at the amount of energy that is required for reactions within a cell. This issue has also been discussed previously in a review by Lee et al. [2]. The summary of their review shows the diversity of the manner in which effect of light was interpreted. However, to this day, no clear solution has been suggested.

Another issue which has been mentioned in previous studies [51], is the difference between indoor and outdoor data. Majority of the models have been derived and tested using indoor data, while outdoor cultures experience entirely different growth conditions. In case of light exposure, while indoor data are collected using artificial lights and under constant irradiance, in an outdoor environment sun is the only source of light and the intensity of this light is constantly changing throughout the day. All these make the results of parameter estimation from an indoor data rather useless for outdoor modelling.

It has been realised through this research that the most critical gap in the majority of the studies is lack of focus on the ultimate application of microalgae. Whether the goal is biofuel or any other product, the production is done outdoor and in large scale and if the model is trying to predict the productivity over a long period of time, a new approach to modelling is needed as some of the effects discussed in the models lose their significance. For instance, as illustrated by Tredici [201] due to light attenuation only a few centimetres of the culture is in the light-saturated zone, while the majority of the culture is photolimited and maybe only a few milimetres in the photoinhibted zone. This implies that the culture as a whole is severely light-limited. In other words, if long-term production data is used, as found by authors in a yet unpublished work, the culture does not experience photosaturation or photoinhibition at a significant level. However, the issue with this approach is the need for a large amount of outdoor data which is an extremely time-consuming task.

3.2. Temperature

The effect of temperature has been studied widely for microalgae and also for other photosynthetic organisms. In most cases its function has been included in the model in the form of multiplication; however, there are some cases where effects of light and temperature were coupled together using more complex functions. When the temperature is solely studied, the growth seems to increase exponentially at first but then it slows down and abruptly declines to zero in a narrow temperature range. This sharp drop is often associated with the death of algal cells due to disruption in the metabolism [202] as a result of deactivation of enzymes or modification of proteins [203]. The short span of declining growth phase imposes limitations in measuring growth between optimum and maximum temperature, as the growth is sensitive to slight temperature variations in this range. Thus, it is more difficult to obtain suitable data points in this range, which result in high uncertainty in parameter estimation [203]. Bernard and Remond [15] found rather large confidence intervals for the cardinal temperatures especially when there was only one data point for growth above optimum temperature. Since the result of parameter estimation and its stability highly depends on the number of data points, the challenge here is to acquire more growth rates at various temperatures specifically at levels higher than optimum temperature.

Temperature also has impacts on chemical reactions and enzymatic activities, which suggest that all other reactions around an algal cell, such as nutrient uptake, will be affected by temperature variations. Moreover, temperature affects pH and also gas absorption in the media which have an influence on growth directly or indirectly. All these suggest that there is still much more to temperature than just its direct effect on growth which needs to be investigated further.

Furthermore, all the reviewed models in this paper describe the growth under constant temperature, but when it comes to variating temperatures, which is the case in outdoor cultures, none of the models is able to explain how algal growth rate reacts to these changes and how fast to they adapt to the new temperature. As we know temperature is changing during the day and despite the fact that temperature variation in the culture is smaller than the air, the temperature fluctuation is significant enough to influence cells activity.

3.3. Temperature and relationship with light

There is no doubt that temperature affects the growth rate, and there is a minimum and a maximum temperature between which growth can take place. Some of the suggested models are accurate but in a narrow range, and some are solely empirical correlations with no theory behind them. There are also many cases where the relationship between temperature and light has been simplified to a multiplication of light and temperature functions [15,72,96,204], while just a few studies coupled the effect of light and temperature in one equation [86,87,97,99]. Furthermore, the effect of temperature on photoinhibition is another issue that has not been widely modelled and in many cases, the photoinhibition effect is overestimated especially when the light intensity at different depths is used to calculate photoinhibition.

As mentioned before lack of validation based on outdoor data is a serious problem in microalgal growth modelling, but what makes the situation more complicated is the fact that in most cases high daily irradiance is associated with higher temperatures. Therefore, when outdoor data is being used it is rather difficult to observe to what extent the change in growth is due to change in irradiance and to what extent due to temperature variation.

In their study, Bechet et al. [51] reviewed various light and temperature models to find the most suitable approach for modelling the outdoor systems. They suggested the use of uncoupled models where the interdependency between light and temperature is neglected. The reason for this suggestion is the complexity of the models for this relationship which may lead to overfitting. However, this approach may cause an error in the prediction if this interdependency is significant.

3.4. Carbon-pH relationship and its effect

Carbon is the primary nutrient for the growth of algal cells, and in dense cultures, it is a limiting factor. It also directly affects pH of the culture which is another important parameter for the growth of the microalgae. Therefore, a good understanding of the relationship between pH and carbon concentration in the medium and also between growth rate and these two parameters is required. The existing models lack a justified relation between these two as all of them used one of these two parameters to determine growth rate. But while carbon

dioxide concentration has a substantial effect on pH of the media it is not the only parameter that manipulates it. The model proposed by Jayaraman and Rhinehart [18] suggests that lower pH results in a higher growth rate which is acceptable to a certain value but further decreasing pH value beyond that point will cause a drop in the growth rate [205]. The approach used by Filali et al. [71] showed better results; however, it used pH solely to calculate the amount of inorganic carbon which was used in a Monod-type model. Hence, high amount of carbon will increase the growth rate in this model and makes it unable to determine an optimum pH for growing microalgae. This suggests that this model may only be applicable in a narrow range of pH. The problem with mentioned models is that even though they show the positive effect of elevated carbon concentration on microalgae growth, they fail to show its adverse effect at very low pH values. Therefore, when only carbon concentration is used, models considering an inhibitory effect for carbon [80,94] are more appropriate. On the other hand, since determining the amount of carbon in a culture can be more difficult than pH, the models using pH are easier to implement. Moreover, the majority of these models are able to predict an optimum pH for growth which means they are considering the limiting effect of high and low pH.

The main issue with the existing models is considering the effect of pH and carbon content as a whole, which is not exactly correct. The reason for this consideration is the use of carbon dioxide injection as a mean for pH control, which ties these parameters together and makes observing the effect of each of them independently impossible. In an attempt to uncouple the pH and carbon content, where the buffer was used to control pH instead of carbon dioxide injection, Bartley et al. [165], observed optimum pH for *Nannochloropsis salina* to be higher than previous studies [206–208]. This may suggest that the reason many researchers find better growth at lower pH levels could be because of the presence of more carbon dioxide. However, more studies seem necessary in this area to approve it, and also to see the effect of pH and carbon content on the growth of microalgae separately.

3.5. Salinity

Salinity is an influential parameter if saline water is to be used for microalgal cultivation. As discussed before, using saline water has multiple advantages when it comes to economy of microalgal systems. The effect of salinity is widely accepted, and some explanations have been provided to clarify the mechanism of this effect [183]. However, no model is proposed including salinity as a parameter and describing the impact of changes in salinity on the growth rate, which leaves this area wide open for investigation and model development. Understanding the effect of salinity on growth not only helps in predicting growth rate but also in designing suitable strategies to maximise productivity while minimising the costs. For instance, implementation of medium recycling causes a constant increase in salinity level of the medium which may make maintaining an optimal level of production difficult. Two strategies are commonly known to overcome this issue. First, starting from microalgae with lower salinity tolerance and as the salinity level rises using the medium for the strains with higher tolerance [174]. The second approach is to use strains of microalgae which have high productivity over a wide range of salinity [209]. Either of these approaches requires a good understanding of the effect of salinity on key production measurements such as growth.

3.6. Indoor vs outdoor

As mentioned before, despite the large number of models that were developed to describe the growth of microalgae, there is no clear evidence suggesting that any of the models are reliable to be used for outdoor cultures. The gap between controlled-condition modelling and real-situation modelling is still significant. This gap can be observed from different aspects. First of all, in a controlled condition usually only one or two process parameters are changing and the rest are kept constant so that observation of the effects of those parameters are more clear and more reliable. Despite being beneficial to see the effect of one process parameter decoupled from other parameters, this approach overlooks how multiple process parameters interact. In a real outdoor condition all the parameters are in constant variation, hence if there is an overlooked interaction between two parameters, the model will not be able to predict reliable values. Moreover, the continuous variation of process parameters is another aspect that has not been included in the models. All the models that are reviewed in this paper found the growth rate based on a constant value of the process parameters which means the model determines a steady-state value for the growth rate. But since in an outdoor condition all the parameters are changing, these models are unable to predict how cells respond to these fluctuations dynamically and how fast do they adapt to a new condition. This issue is valid for all the process parameters and hence makes modelling more challenging. Acclimation is a major phenomenon in microalgae. As the process conditions change, the cells try to adapt to the new condition. In a more complicated situation, a major factor such as light varies at different locations in a culture. As discussed before, at each time the majority of the culture is light-limited which causes cells to adapt to low light intensity. Therefore, when they are exposed to regions with high irradiance, they do not use the light efficiently [201]. If the modelling is based on long-term outdoor data, acclimation will become less of an issue, as for some outdoor conditions, such as irradiance and temperature, the average over an extended period hardly changes radically but often in a gradual manner by changes in the seasons. So the cells have already been provided sufficient time to adapt to the new condition which facilitates the modelling process. Finally, to make it more complicated, we need to realise that hydrodynamics in a culture also play a major role in the conditions each cell experiences which has a significant effect on the light history of cells, absorption of carbon dioxide from atmosphere and release of produced oxygen.

3.7. Comprehensive growth models

A comprehensive growth model is a model that takes into account the effect of multiple process parameters to predict growth rate under outdoor conditions and lack of such a model is noticeable. There are major challenges in the path to a successful comprehensive model. These models tie various process parameters together and as the number of the process parameters increase the model becomes more difficult to validate. Having more process parameters is associated with having more model constants which implies that massive amount of data is required for parameter estimation and model validation. Obtaining datasets large enough to properly serve such a model may require extensive time and resources.

Having a large number of constants in a model also causes another issue with the model called overfitting. Overfitting happens due to high degree of freedom in a model as a result of numerous model constants and makes the result of parameter estimation unreliable even if the model produces a low error in its predictions. Commonly, as a result of overfitting, the model may converge to unrealistic values for its constants and when tested against a second set of data for validation, it may result in significantly larger error values.

4. Practical implications of this study

Modelling a biological system is a challenging task since there are thousands of reactions involved within each cell to be included. The typical mindset towards modelling such systems is to model general characteristics of the system without getting involved in too much detail of cell metabolism. There are numerous metabolic reactions involved, and the data needed to model them are often difficult to obtain which makes such modelling practically impossible. The majority of the models discussed in this paper tried to model a microalgal system based

on indoor laboratory data. However, since one of the goals of using microalgae is for commercial production, focusing on indoor data seems impractical. There are numerous effects to be included in the modelling which is another main challenge. However, by changing the focus from short-term indoor data to long-term outdoor, some of the issues could be resolved or ameliorated. An excellent example of this difference is the importance of acclimation which is crucial in short-term but insignificant in long-term studies.

Moreover, outdoor data comes with its specific pattern that could potentially facilitate modelling. For instance, light and temperature variation throughout a day follows a particular pattern with minor changes due to weather conditions. An ideal short-term model would be able to predict the influence of these changes on the growth, but as discussed before, developing such a model is a difficult task. On the other hand, long-term modelling can resolve the issue since the average over an extended period changes gradually and commonly does not have drastic fluctuations. Although, the short term modelling has the potential to provide more accurate results, in reality, long-term modelling can provide solutions that are easier to develop and to apply. A demonstration of this approach can be seen in the authors' previous works [210,211].

Salinity is another factor that has a significant role in practice. As discussed earlier, using saline water in the form of seawater or saline underground water facilitates the provision of water where there is little access to freshwater. More importantly, it considerably reduces the total cost of production. The cost of maintaining a microalgae culture is rather high, and any step in lowering the cost is an advancement towards a viable production. Using saline water, however, requires a good understanding of the relationship between salinity of the medium and production indicators such as growth. A model to describe this relationship is still missing from the literature, having which could improve the predictions for productivity and profitability of an algal system.

5. Conclusion

A review of available models considering the effects of light, temperature, nutrients, pH, carbon concentration, and oxygen on the growth of microalgae is presented. Salinity is one of the key parameters in the growth of marine algae which has not been considered in the modelling so far. There is clear evidence to show the benefits of using saline water for growing microalgae, but due to evaporation and recycling, the salinity of the media will increase continuously if such type of water is used. Therefore, it is vital to model the effect of salinity on growth in order to achieve a practical model for microalgal production. Also, as discussed before in a review by Bechet et al. [51], when it comes to outdoor cultivation, not many models have been validated for this condition. Even if a model has performed well on laboratory data, given that outdoor cultivation is associated with a different source of light and many uncontrollable conditions, its reliability is still questionable. This issue is more significant when it comes to the effect of light as by nature the artificial light sources that are used in the labs have different spectra and intensity compared to sunlight. Thus, a validation using outdoor data is necessary for the models to certify their usability in a real condition. Additionally, these conditions fluctuate regularly and this behaviour is not included in most of the models. If a model is going to be used for outdoor data, especially when the model is used for process control, predicting its response to the variations in process conditions is critical. Modelling the effects of these variations on growth is an extremely difficult task. However, if modelling is done for a longer period, instead of the instantaneous response to changes, some of the issues may not be valid as they affect short-term growth and not long-term. For instance, the specific growth rate of a culture within a week or a fortnight can sum up the effects of process conditions and neglect the small variations which are insignificant in large scales.

Furthermore, the majority of the discussed models were designed to consider the effect of only one or two parameters while in reality, all the mentioned parameters will be playing a notable role in the growth. Therefore, a combination of various models is needed to form a comprehensive model which can predict growth under various changes in the process conditions. However, developing a comprehensive model itself will bring up new issues as these models have a large number of constants and require extensive experimental data for parameter estimation and validation. Overfitting is another common issue when the number of model constants grows. However, one way to avoid these issues to some extent, is by studying a culture as bulk and in wider timeframes. This means instead of studying the effect of the parameters at different depths, and within small time intervals, the overall performance of a model can be studied for a culture in longer periods. Moreover, outdoor cultures usually experience a more or less same pattern of conditions. For instance, the changes in light and temperature within a day is generally similar in most days with only slight changes due to the day of the year and weather conditions . Furthermore, in long-term, the range in which a certain process parameter varies is not wide. Daily solar irradiance for a particular location is within a relatively narrow range, and therefore it is unnecessary to model the effect of irradiance for a broad range. These patterns and correlations between process parameters can be helpful in simplification of the models and construction of a model with a lower number of constants which would be easier to apply and verify. Such a model may not have the meaningfulness of the detailed mechanistic models in terms of formulating what happens inside a cell, but it may be more applicable in large scale cultures and for long-term cultivation of microalgae.

References

[1] Kumar A, Ergas S, Yuan X, Sahu A, Zhang Q, Dewulf J, et al. Enhanced CO_2 fixation and biofuel production via microalgae: recent developments and future directions. Trends Biotechnol 2010;28:371–80.
[2] Lee E, Jalalizadeh M, Zhang Q. Growth kinetic models for microalgae cultivation: a review. Algal Res 2015;12:497–512.
[3] Concas A, Pisu M, Cao G. A novel mathematical model to simulate the size-structured growth of microalgae strains dividing by multiple fission. Chem Eng J 2016;287:252–68.
[4] Salama E-S, Kurade MB, RaI Abou-Shanab, El-Dalatony MM, Yang I-S, Min B, et al. Recent progress in microalgal biomass production coupled with wastewater treatment for biofuel generation. Renew Sustain Energy Rev 2017;79:1189–211.
[5] Batista AP, Ambrosano L, Graça S, Sousa C, Marques PaSS, Ribeiro B, et al. Combining urban wastewater treatment with biohydrogen production – an integrated microalgae-based approach. Bioresour Technol 2015;184:230–5.
[6] Kligerman DC, Bouwer EJ. Prospects for biodiesel production from algae-based wastewater treatment in Brazil: a review. Renew Sustain Energy Rev 2015;52:1834–46.
[7] Borowitzka MA, Moheimani NR. Sustainable biofuels from algae. Mitig Adapt Strateg Glob Change 2013;18:13–25.
[8] Mata TM, Martins AA, Caetano NS. Microalgae for biodiesel production and other applications: a review. Renew Sustain Energy Rev 2010;14:217–32.
[9] Zeng X, Danquah MK, Chen XD, Lu Y. Microalgae bioengineering: from CO_2 fixation to biofuel production. Renew Sustain Energy Rev 2011;15:3252–60.
[10] Chang H-X, Huang Y, Fu Q, Liao Q, Zhu X. Kinetic characteristics and modeling of microalgae Chlorella vulgaris growth and CO_2 biofixation considering the coupled effects of light intensity and dissolved inorganic carbon. Bioresour Technol 2016;206:231–8.
[11] Nikolaou A, Hartmann P, Sciandra A, Chachuat B, Bernard O. Dynamic coupling of photoacclimation and photoinhibition in a model of microalgae growth. J Theor Biol 2016;390:61–72.
[12] Ippoliti D, Gómez C, Del Mar Morales-Amaral M, Pistocchi R, Fernández-Sevilla J, Acién FG. Modeling of photosynthesis and respiration rate for Isochrysis galbana (T-Iso) and its influence on the production of this strain. Bioresour Technol 2016;203:71–9.
[13] Spolaore P, Joannis-Cassan C, Duran E, Isambert A. Commercial applications of microalgae. J Biosci Bioeng 2006;101:87–96.
[14] Tramontin DP, Gressler PD, Rörig LR, Derner RB, Pereira-Filho J, Radetski CM, et al. Growth modeling of the green microalga Scenedesmus obliquus in a hybrid photobioreactor as a practical tool to understand both physical and biochemical phenomena in play during algae cultivation. Biotechnol Bioeng 2017.
[15] Bernard O, Rémond B. Validation of a simple model accounting for light and temperature effect on microalgal growth. Bioresour Technol 2012;123:520–7.
[16] Khan SA, Rashmi, Hussain MZ, Prasad S, Banerjee UC. Prospects of biodiesel production from microalgae in India. Renew Sustain Energy Rev 2009;13:2361–72.

[17] Huang Y, Su C. High lipid content and productivity of microalgae cultivating under elevated carbon dioxide. Int J Environ Sci Technol 2014;11:703–10.
[18] Jayaraman SK, Rhinehart RR. Modeling and optimization of algae growth. Ind Eng Chem Res 2015;54:8063–71.
[19] Chisti Y. Constraints to commercialization of algal fuels. J Biotechnol 2013;167:201–14.
[20] Ugwu CU, Aoyagi H, Uchiyama H. Photobioreactors for mass cultivation of algae. Bioresour Technol 2008;99:4021–8.
[21] Richardson JW, Johnson MD, Zhang X, Zemke P, Chen W, Hu Q. A financial assessment of two alternative cultivation systems and their contributions to algae biofuel economic viability. Algal Res 2014;4:96–104.
[22] Bernard O, Mairet F, Chachuat B. Modelling of microalgae culture systems with applications to control and optimization. Microalgae Biotechnol 2015:59–87.
[23] Benson BC, Rusch KA. Investigation of the light dynamics and their impact on algal growth rate in a hydraulically integrated serial turbidostat algal reactor (HISTAR). Aquac Eng 2006;35:122–34.
[24] Huesemann MH, Van Wagenen J, Miller T, Chavis A, Hobbs S, Crowe B. A screening model to predict microalgae biomass growth in photobioreactors and raceway ponds. Biotechnol Bioeng 2013;110:1583–94.
[25] Bernard O. Hurdles and challenges for modelling and control of microalgae for CO_2 mitigation and biofuel production. J Process Control 2011;21:1378–89.
[26] Yuan S, Zhou X, Chen R, Song B. Study on modelling microalgae growth in nitrogen-limited culture system for estimating biomass productivity. Renew Sustain Energy Rev 2014;34:525–35.
[27] Blanken W, Postma PR, De Winter L, Wijffels RH, Janssen M. Predicting microalgae growth. Algal Res 2016;14:28–38.
[28] Molina Grima E, Garcia Camacho F, Sanchez Perez JA, Fernandez Sevilla JM, Acien Fernandez FG, Contreras Gomez A. A mathematical model of microalgal growth in light-limited chemostat culture. J Chem Technol Biotechnol 1994;61:167–73.
[29] Packer A, Li Y, Andersen T, Hu Q, Kuang Y, Sommerfeld M. Growth and neutral lipid synthesis in green microalgae: a mathematical model. Bioresour Technol 2011;102:111–7.
[30] Sukenik A, Falkowski P, Bennett J. Potential enhancement of photosynthetic energy conversion in algal mass culture. Biotechnol Bioeng 1987;30:970–7.
[31] Cornet JF, Dussap CG, Gros JB, Binois C, Lasseur C. A simplified monodimensional approach for modeling coupling between radiant light transfer and growth kinetics in photobioreactors. Chem Eng Sci 1995;50:1489–500.
[32] Cornet JF, Dussap CG. A simple and reliable formula for assessment of maximum volumetric productivities in photobioreactors. Biotechnol Prog 2009;25:424–35.
[33] Lee HY, Erickson LE, Yang SS. Kinetics and bioenergetics of light-limited photoautotrophic growth of Spirulina platensis. Biotechnol Bioeng 1987;29:832–43.
[34] Aiba S. Growth kinetics of photosynthetic microorganisms. Adv Biochem Eng 1982;23:85–156.
[35] Han BP, Virtanen M, Koponen J, Straškraba M. Effect of photoinhibition on algal photosynthesis: a dynamic model. J Plankton Res 2000;22:865–85.
[36] Baly E. The kinetics of photosynthesis. Proc R Soc Lond Ser B Biol Sci 1935;117:218–39.
[37] Tamiya H, Hase E, Shibata K, Mituya A, Iwamura T, Nihei T, et al. Kinetics of growth of Chlorella, with special reference to its dependence on quantity of available light and on temperature. Algal Cult Lab Pilot Plant 1953:204–32.
[38] Monod J. The growth of bacterial cultures. Annu Rev Microbiol 1949;3:371–94.
[39] Smith EL. Photosynthesis in relation to light and carbon dioxide. Proc Natl Acad Sci USA 1936;22:504.
[40] Bannister TT. Quantitative description of steady state, nutrient-saturated algal growth, including adaptation. Limnol Oceanogr 1979;24:76–96.
[41] Myers J, Graham J-R. The photosynthetic unit in Chlorella measured by repetitive short flashes. Plant Physiol 1971;48:282–6.
[42] Myers J, Graham J-R. Enhancement in Chlorella. Plant Physiol 1963;38:105.
[43] Nielsen ES, Jørgensen EG. The adaptation of plankton algae. Physiol Plant 1968;21:401–13.
[44] Jorgensen EG. Adaptation to different light intensities in the diatom Cyclotella Meneghiniana Kütz. Physiol Plant 1964;17:136–45.
[45] Nielsen ES. Inactivation of the photochemical mechanism in photosynthesis as a means to protect the cells against too high light intensities. Physiol Plant 1962;15:161–71.
[46] Jassby AD, Platt T. Mathematical formulation of the relationship between photosynthesis and light for phytoplankton. Limnol Oceanogr 1976;21:540–7.
[47] Platt T, Jassby AD. The relationship between photosynthesis and light for natural assemblages of coastal marine phytoplankton. J Phycol 1976;12:421–30.
[48] Chalker BE. Modeling light saturation curves for photosynthesis: an exponential function. J Theor Biol 1980;84:205–15.
[49] Van Oorschot JLP. Conversion of light energy in algal culture; 1955.
[50] Powles SB. Photoinhibition of photosynthesis induced by visible light. Annu Rev Plant Physiol 1984;35:15–44.
[51] Béchet Q, Shilton A, Guieysse B. Modeling the effects of light and temperature on algae growth: state of the art and critical assessment for productivity prediction during outdoor cultivation. Biotechnol Adv 2013;31:1648–63.
[52] Steele JH. Environmental control of photosynthesis in the sea. Limnol Oceanogr 1962;7:137–50.
[53] Crill PA. The photosynthesis-light curve: a simple analog model. J Theor Biol 1977;64:503–16.
[54] Peeters J, Eilers P. The relationship between light intensity and photosynthesis—a simple mathematical model. Hydrobiol Bull 1978;12:134–6.
[55] Megard RO, Tonkyn DW, Senft WH. Kinetics of oxygenic photosynthesis in planktonic algae. J Plankton Res 1984;6:325–37.
[56] Eilers PHC, Peeters JCH. A model for the relationship between light intensity and the rate of photosynthesis in phytoplankton. Ecol Model 1988;42:199–215.
[57] Eilers PHC, Peeters JCH. Dynamic behaviour of a model for photosynthesis and photoinhibition. Ecol Model 1993;69:113–33.
[58] Dauta A, Devaux J, Piquemal F, Boumnich L. Growth rate of four freshwater algae in relation to light and temperature. Hydrobiologia 1990;207:221–6.
[59] Molina Grima E, Fernández Sevilla JM, Sánchez Pérez JA, García Camacho F. A study on simultaneous photolimitation and photoinhibition in dense microalgal cultures taking into account incident and averaged irradiances. J Biotechnol 1996;45:59–69.
[60] García-Malea MC, Acién FG, Fernández JM, Cerón MC, Molina E. Continuous production of green cells of Haematococcus pluvialis: modeling of the irradiance effect. Enzym Microb Technol 2006;38:981–9.
[61] Wu X, Merchuk JC. Simulation of algae growth in a bench-scale bubble column reactor. Biotechnol Bioeng 2002;80:156–68.
[62] Wu X, Merchuk JC. Simulation of algae growth in a bench scale internal loop airlift reactor. Chem Eng Sci 2004;59:2899–912.
[63] Rubio Camacho F, García Camacho F, Fernández Sevilla JM, Chisti Y, Molina Grima E. A mechanistic model of photosynthesis in microalgae. Biotechnol Bioeng 2003;81:459–73.
[64] Ritchie R. Modelling photosynthetic photon flux density and maximum potential gross photosynthesis. Photosynthetica 2010;48:596–609.
[65] Mccree KJ. The action spectrum, absorptance and quantum yield of photosynthesis in crop plants. Agric Meteorol 1971;9:191–216.
[66] Holzinger A, Lütz C. Algae and UV irradiation: effects on ultrastructure and related metabolic functions. Micron 2006;37:190–207.
[67] Wiencke C, Gómez I, Pakker H, Flores-Moya A, Altamirano M, Hanelt D, et al. Impact of UV-radiation on viability, photosynthetic characteristics and DNA of brown algal zoospores: implications for depth zonation. Mar Ecol Prog Ser 2000:217–29.
[68] Wiencke C, Clayton M, Schoenwaelder M. Sensitivity and acclimation to UV radiation of zoospores from five species of Laminariales from the Arctic. Mar Biol 2004;145:31–9.
[69] Jeon YC, Cho CW, Yun YS. Measurement of microalgal photosynthetic activity depending on light intensity and quality. Biochem Eng J 2005;27:127–31.
[70] Haario H, Kalachev L, Laine M. Reduced models of algae growth. Bull Math Biol 2009;71:1626–48.
[71] Filali R, Tebbani S, Dumur D, Isambert A, Pareau D, Lopes F. Growth modeling of the green microalga Chlorella vulgaris in an air-lift photobioreactor. TIC 2011:10.
[72] Franz A, Lehr F, Posten C, Schaub G. Modeling microalgae cultivation productivities in different geographic locations - estimation method for idealized photobioreactors. Biotechnol J 2012;7:546–57.
[73] Ifrim GA, Titica M, Cogne G, Boillereaux L, Legrand J, Caraman S. Dynamic pH model for autotrophic growth of microalgae in photobioreactor: a tool for monitoring and control purposes. AIChE J 2014;60:585–99.
[74] Béchet Q, Chambonnière P, Shilton A, Guizard G, Guieysse B. Algal productivity modeling: a step toward accurate assessments of full-scale algal cultivation. Biotechnol Bioeng 2015;112:987–96.
[75] Kasiri S, Ulrich A, Prasad V. Kinetic modeling and optimization of carbon dioxide fixation using microalgae cultivated in oil-sands process water. Chem Eng Sci 2015;137:697–711.
[76] Lee E, Zhang Q. Integrated co-limitation kinetic model for microalgae growth in anaerobically digested municipal sludge centrate. Algal Res 2016;18:15–24.
[77] Laws EA, Chalup MS. A microalgal growth model. Limnol Oceanogr 1990;35:597–608.
[78] Grima EM, Pérez JS, Camacho FG, Sánchez JG, Alonso DL. n-3 PUFA productivity in chemostat cultures of microalgae. Appl Microbiol Biotechnol 1993;38:599–605.
[79] Concas A, Pisu M, Cao G. Novel simulation model of the solar collector of BIOCOIL photobioreactors for CO_2 sequestration with microalgae. Chem Eng J 2010;157:297–303.
[80] Pegallapati AK, Nirmalakhandan N. Modeling algal growth in bubble columns under sparging with CO_2-enriched air. Bioresour Technol 2012;124:137–45.
[81] Fernández I, Acién F, Fernández J, Guzmán J, Magán J, Berenguel M. Dynamic model of microalgal production in tubular photobioreactors. Bioresour Technol 2012;126:172–81.
[82] Costache T, Fernández FGA, Morales M, Fernández-Sevilla J, Stamatin I, Molina E. Comprehensive model of microalgae photosynthesis rate as a function of culture conditions in photobioreactors. Appl Microbiol Biotechnol 2013;97:7627–37.
[83] Fernández I, Acién F, Guzmán J, Berenguel M, Mendoza J. Dynamic model of an industrial raceway reactor for microalgae production. Algal Res 2016;17:67–78.
[84] Fouchard S, Pruvost J, Degrenne B, Titica M, Legrand J. Kinetic modeling of light limitation and sulfur deprivation effects in the induction of hydrogen production with Chlamydomonas reinhardtii: Part I. Model development and parameter identification. Biotechnol Bioeng 2009;102:232–45.
[85] Mirzaie MM, Kalbasi M, Ghobadian B, Mousavi S. Kinetic modeling of mixotrophic growth of Chlorella vulgaris as a new feedstock for biolubricant. J Appl Phycol 2016:1–11.
[86] Talbot P, Thébault J-M, Dauta A, De La, Noüe J. A comparative study and mathematical modeling of temperature, light and growth of three microalgae potentially useful for wastewater treatment. Water Res 1991;25:465–72.
[87] Dermoun D, Chaumont D, Thebault JM, Dauta A. Modelling of growth of Porphyridium cruentum in connection with two interdependent factors: light and temperature. Bioresour Technol 1992;42:113–7.
[88] Grobbelaar JU, Soeder CJ, Stengel E. Modeling algal productivity in large outdoor cultures and waste treatment systems. Biomass 1990;21:297–314.
[89] Munoz-Tamayo R, Martinon P, Bougaran G, Mairet F, Bernard O. Getting the most

out of it: optimal experiments for parameter estimation of microalgae growth models. J Process Control 2014;24:991–1001.
[90] Ogbonna JC, Yada H, Tanaka H. Kinetic study on light-limited batch cultivation of photosynthetic cells. J Ferment Bioeng 1995;80:259–64.
[91] Geider RJ, Macintyre HL, Kana TM. Dynamic model of phytoplankton growth and acclimation: responses of the balanced growth rate and the chlorophyll a: carbon ratio to light, nutrient-limitation and temperature. Mar Ecol Prog Ser 1997;148:187–200.
[92] Geider RJ, Macintyre HL, Kana TM. A dynamic regulatory model of phytoplanktonic acclimation to light, nutrients, and temperature. Limnol Oceanogr 1998;43:679–94.
[93] Meseck SL, Alix JH, Wikfors GH. Photoperiod and light intensity effects on growth and utilization of nutrients by the aquaculture feed microalga, Tetraselmis chui (PLY429). Aquaculture 2005;246:393–404.
[94] Baquerisse D, Nouals S, Isambert A, Dos Santos PF, Durand G. Modelling of a continuous pilot photobioreactor for microalgae production. J Biotechnol 1999;70:335–42.
[95] James SC, Boriah V. Modeling algae growth in an open-channel raceway. J Comput Biol 2010;17:895–906.
[96] Marsullo M, Mian A, Ensinas AV, Manente G, Lazzaretto A, Marechal F. Dynamic modeling of the microalgae cultivation phase for energy production in open raceway ponds and flat panel photobioreactors. Front Energy Res 2015;3:41.
[97] Collins CD, Boylen CW. Physiological responses of Anabaena variabilis (Cyanophyceae) to instantaneous exposure to various combinations of light intensity and temperature. J Phycol 1982;18:206–11.
[98] Guterman H, Vonshak A, Ben-Yaakov S. A macromodel for outdoor algal mass production. Biotechnol Bioeng 1990;35:809–19.
[99] Carvalho AP, Malcata FX. Kinetic modeling of the autotrophic growth of Pavlova lutheri: study of the combined influence of light and temperature. Biotechnol Prog 2003;19:1128–35.
[100] Muller-Feuga A. Growth as a function of rationing: a model applicable to fish and microalgae. J Exp Mar Biol Ecol 1999;236:1–13.
[101] Klausmeier CA, Litchman E, Levin SA. Phytoplankton growth and stoichiometry under multiple nutrient limitation. Limnol Oceanogr 2004;49:1463–70.
[102] Converti A, Casazza AA, Ortiz EY, Perego P, Del Borghi M. Effect of temperature and nitrogen concentration on the growth and lipid content of Nannochloropsis oculata and Chlorella vulgaris for biodiesel production. Chem Eng Process: Process Intensif 2009;48:1146–51.
[103] Chen M, Tang H, Ma H, Holland TC, Ng KS, Salley SO. Effect of nutrients on growth and lipid accumulation in the green algae Dunaliella tertiolecta. Bioresour Technol 2011;102:1649–55.
[104] Goldman JC, Oswald WJ, Jenkins D. The kinetics of inorganic carbon limited algal growth. J Water Pollut Control Fed 1974:46.
[105] Hsueh HT, Li WJ, Chen HH, Chu H. Carbon bio-fixation by photosynthesis of Thermosynechococcus sp. CL-1 and Nannochloropsis oculta. J Photochem Photobiol B: Biol 2009;95:33–9.
[106] Aslan S, Kapdan IK. Batch kinetics of nitrogen and phosphorus removal from synthetic wastewater by algae. Ecol Eng 2006;28:64–70.
[107] Xin L, Hong-Ying H, Ke G, Ying-Xue S. Effects of different nitrogen and phosphorus concentrations on the growth, nutrient uptake, and lipid accumulation of a freshwater microalga Scenedesmus sp. Bioresour Technol 2010;101:5494–500.
[108] Andrews JF. A mathematical model for the continuous culture of microorganisms utilizing inhibitory substrates. Biotechnol Bioeng 1968;10:707–23.
[109] Caperon J. Population growth response of Isochrysis galbana to nitrate variation at limiting concentrations. Ecology 1968:866–72.
[110] Droop MR. Vitamin B12 and marine ecology, IV. The kinetics of uptake, growth and inhibition in Monochrysis lutheri. J Mar Biol Assoc UK 1968;48:689–733.
[111] Flynn KJ. How critical is the critical N:P ratio? J Phycol 2002;38:961–70.
[112] Martínez Sancho ME, Castillo JMJ, El Yousfi F. Influence of phosphorus concentration on the growth kinetics and stoichiometry of the microalga Scenedesmus obliquus. Process Biochem 1997;32:657–64.
[113] Martínez ME, Jiménez JM, El Yousfi F. Influence of phosphorus concentration and temperature on growth and phosphorus uptake by the microalga Scenedesmus obliquus. Bioresour Technol 1999;67:233–40.
[114] Droop M. The nutrient status of algal cells in continuous culture. J Mar Biol Assoc UK 1974;54:825–55.
[115] Droop M. The nutrient status of algal cells in batch culture. J Mar Biol Assoc UK 1975;55:541–55.
[116] Quinn J, De Winter L, Bradley T. Microalgae bulk growth model with application to industrial scale systems. Bioresour Technol 2011;102:5083–92.
[117] Grover JP. Dynamics of competition among microalgae in variable environments: experimental tests of alternative models. Oikos 1991;62:231–43.
[118] Sunda W, Shertzer K, Hardison D. Ammonium uptake and growth models in marine diatoms: Monod and Droop revisited. Mar Ecol Prog Ser 2009;386:29–41.
[119] Adesanya VO, Davey MP, Scott SA, Smith AG. Kinetic modelling of growth and storage molecule production in microalgae under mixotrophic and autotrophic conditions. Bioresour Technol 2014;157:293–304.
[120] Bougaran G, Bernard O, Sciandra A. Modeling continuous cultures of microalgae colimited by nitrogen and phosphorus. J Theor Biol 2010;265:443–54.
[121] Sommer U. A comparison of the Droop and the Monod models of nutrient limited growth applied to natural populations of phytoplankton. Funct Ecol 1991:535–44.
[122] Caperon J, Meyer J. Nitrogen-limited growth of marine phytoplankton-I. changes in population characteristics with steady-state growth rate. Deep-Sea Res Oceanogr Abstr 1972;19:601–18.
[123] Caperon J, Meyer J. Nitrogen-limited growth of marine phytoplankton-II. Uptake kinetics and their role in nutrient limited growth of phytoplankton. Deep-Sea Res Oceanogr Abstr 1972;19:619–32.
[124] Droop M. Some thoughts on nutrient limitation in algae. J Phycol 1973;9:264–72.
[125] Goldman JC, Mccarthy JJ. Steady state growth and ammonium uptake of a fast-growing marine diatom. Limnol Oceanogr 1978;23:695–703.
[126] Guest JS, Van Loosdrecht MCM, Skerlos SJ, Love NG. Lumped pathway metabolic model of organic carbon accumulation and mobilization by the alga Chlamydomonas reinhardtii. Environ Sci Technol 2013;47:3258–67.
[127] Haefner JW. Modeling biological systems: principles and applications. New York: Springer Science & Business Media; 2005. ISBN-10:0-387-25012-3.
[128] O'neill R, Deangelis D, Pastor J, Jackson B, Post W. Multiple nutrient limitations in ecological models. Ecol Model 1989;46:147–63.
[129] Spijkerman E, De Castro F, Gaedke U. Independent colimitation for carbon dioxide and inorganic phosphorus. PLoS One 2011;6:e28219.
[130] Chen M, Fan M, Liu R, Wang X, Yuan X, Zhu H. The dynamics of temperature and light on the growth of phytoplankton. J Theor Biol 2015;385:8–19.
[131] Fré NCD, Chagas ALD, Rech R, Marcílio NR. Kinetic modeling of Dunaliella tertiolecta growth under different nitrogen concentrations. Chem Eng Technol 2016.
[132] Zhang X-W, Chen F, Johns MR. Kinetic models for heterotrophic growth of Chlamydomonas reinhardtii in batch and fed-batch cultures. Process Biochem 1999;35:385–9.
[133] Burmaster DE. The unsteady continuous culture of phosphate-limited Monochrysis lutheri Droop: experimental and theoretical analysis. J Exp Mar Biol Ecol 1979;39:167–86.
[134] Wu Y-H, Li X, Yu Y, Hu H-Y, Zhang T-Y, Li F-M. An integrated microalgal growth model and its application to optimize the biomass production of Scenedesmus sp. LX1 in open pond under the nutrient level of domestic secondary effluent. Bioresour Technol 2013;144:445–51.
[135] Chapelle A, Labry C, Sourisseau M, Lebreton C, Youenou A, Crassous MP. Alexandrium minutum growth controlled by phosphorus. An applied model. J Mar Syst 2010;83:181–91.
[136] De La Hoz Siegler H, Ben-Zvi A, Burrell R, Mccaffrey W. The dynamics of heterotrophic algal cultures. Bioresour Technol 2011;102:5764–74.
[137] De La Hoz Siegler H, Mccaffrey W, Burrell R, Ben-Zvi A. Optimization of microalgal productivity using an adaptive, non-linear model based strategy. Bioresour Technol 2012;104:537–46.
[138] Abdollahi J, Dubljevic S. Lipid production optimization and optimal control of heterotrophic microalgae fed-batch bioreactor. Chem Eng Sci 2012;84:619–27.
[139] He Y, Chen L, Zhou Y, Chen H, Zhou X, Cai F, et al. Analysis and model delineation of marine microalgae growth and lipid accumulation in flat-plate photobioreactor. Biochem Eng J 2016;111:108–16.
[140] Tevatia R, Demirel Y, Blum P. Kinetic modeling of photoautotropic growth and neutral lipid accumulation in terms of ammonium concentration in Chlamydomonas reinhardtii. Bioresour Technol 2012;119:419–24.
[141] Rosso L, Lobry J, Flandrois J. An unexpected correlation between cardinal temperatures of microbial growth highlighted by a new model. J Theor Biol 1993;162:447–63.
[142] Ratkowsky D, Olley J, Mcmeekin T, Ball A. Relationship between temperature and growth rate of bacterial cultures. J Bacteriol 1982;149:1–5.
[143] Ratkowsky D, Lowry R, Mcmeekin T, Stokes A, Chandler R. Model for bacterial culture growth rate throughout the entire biokinetic temperature range. J Bacteriol 1983;154:1222–6.
[144] Sharpe PJ, Curry GL, Demichele DW, Cole CL. Distribution model of organism development times. J Theor Biol 1977;66:21–38.
[145] Sharpe PJ, Demichele DW. Reaction kinetics of poikilotherm development. J Theor Biol 1977;64:649–70.
[146] Schoolfield R, Sharpe P, Magnuson C. Non-linear regression of biological temperature-dependent rate models based on absolute reaction-rate theory. J Theor Biol 1981;88:719–31.
[147] Zwietering M, De Koos J, Hasenack B, De Witt J, Van't Riet K. Modeling of bacterial growth as a function of temperature. Appl Environ Microbiol 1991;57:1094–101.
[148] Lobry J, Rosso L, Flandrois J. A FORTRAN subroutine for the determination of parameter confidence limits in non-linear models. Binary 1991;3:25.
[149] Yan W, Hunt L. An equation for modelling the temperature response of plants using only the cardinal temperatures. Ann Bot 1999;84:607–14.
[150] Yin X, Kropff MJ, Mclaren G, Visperas RM. A nonlinear model for crop development as a function of temperature. Agric For Meteorol 1995;77:1–16.
[151] Gao L, Jin Z, Huang Y, Zhang L. Rice clock model—a computer model to simulate rice development. Agric For Meteorol 1992;60:1–16.
[152] Blanchard GF, Guarini JM, Richard P, Gros P, Mornet F. Quantifying the short-term temperature effect on light-saturated photosynthesis of intertidal microphytobenthos. Mar Ecol Prog Ser 1996;134:309–13.
[153] Eppley RW. Temperature and phytoplankton growth in the sea. Fish Bull 1972;70:1063–85.
[154] Ketheesan B, Nirmalakhandan N. Modeling microalgal growth in an airlift-driven raceway reactor. Bioresour Technol 2013;136:689–96.
[155] Butterwick C, Heaney SI, Talling JF. Diversity in the influence of temperature on the growth rates of freshwater algae, and its ecological relevance. Freshw Biol 2005;50:291–300.
[156] Sukenik A, Levy R, Levy Y, Falkowski P, Dubinsky Z. Optimizing algal biomass production in an outdoor pond: a simulation model. J Appl Phycol 1991;3:191–201.
[157] James SC, Janardhanam V, Hanson DT. Simulating pH effects in an algal-growth hydrodynamics model1. J Phycol 2013;49:608–15.
[158] Bitaubé Pérez E, Caro Pina I, Pérez Rodríguez L. Kinetic model for growth of Phaeodactylum tricornutum in intensive culture photobioreactor. Biochem Eng J

2008;40:520–5.
[159] Tevatia R, Demirel Y, Rudrappa D, Blum P. Effects of thermodynamically coupled reaction diffusion in microalgae growth and lipid accumulation: model development and stability analysis. Comput Chem Eng 2015;75:28–39.
[160] Moisan JR, Moisan TA, Abbott MR. Modelling the effect of temperature on the maximum growth rates of phytoplankton populations. Ecol Model 2002;153:197–215.
[161] Norberg J. Biodiversity and ecosystem functioning: a complex adaptive systems approach. Limnol Oceanogr 2004;49:1269–77.
[162] Rarrek A, Mostertz M, Kistenmacher H, Rehfeldt S, Klein H. Simulation and optimization of large open algae ponds. Chem Eng Res Des 2016;114:220–35.
[163] Slegers P, Lösing M, Wijffels R, Van Straten G, Van Boxtel A. Scenario evaluation of open pond microalgae production. Algal Res 2013;2:358–68.
[164] Moheimani NR, Borowitzka MA. Increased CO_2 and the effect of pH on growth and calcification of Pleurochrysis carterae and Emiliania huxleyi (Haptophyta) in semicontinuous cultures. Appl Microbiol Biotechnol 2011;90:1399–407.
[165] Bartley ML, Boeing WJ, Dungan BN, Holguin FO, Schaub T. pH effects on growth and lipid accumulation of the biofuel microalgae Nannochloropsis salina and invading organisms. J Appl Phycol 2014;26:1431–7.
[166] Moheimani NR. Inorganic carbon and pH effect on growth and lipid productivity of Tetraselmis suecica and Chlorella sp (Chlorophyta) grown outdoors in bag photobioreactors. J Appl Phycol 2013;25:387–98.
[167] Hoh D, Watson S, Kan E. Algal biofilm reactors for integrated wastewater treatment and biofuel production: a review. Chem Eng J 2016;287:466–73.
[168] King DL, Novak JT. The kinetics of inorganic carbon-limited algal growth. J (Water Pollut Control Fed) 1974:1812–6.
[169] Bailey JE, Ollis DF. Biochemical engineering fundamentals. Chem Eng Educ 1976.
[170] Tang I, Okos MR, Yang ST. Effects of pH and acetic acid on homoacetic fermentation of lactate by Clostridium formicoaceticum. Biotechnol Bioeng 1989;34:1063–74.
[171] Ifrim GA, Barbu M, Ceanga E, Caraman S. Modeling and control of a multipurpose biotechnological plant. Photobioreactor modeling. In: Proceedings of the system theory, control and computing (ICSTCC) 2015 19th international conference on: IEEE; 2015, p. 55–60.
[172] Yang J, Xu M, Zhang X, Hu Q, Sommerfeld M, Chen Y. Life-cycle analysis on biodiesel production from microalgae: water footprint and nutrients balance. Bioresour Technol 2011;102:159–65.
[173] Ishika T, Moheimani NR, Bahri PA. Sustainable saline microalgae co-cultivation for biofuel production: a critical review. Renew Sustain Energy Rev 2017;78:356–68.
[174] Ishika T, Bahri PA, Laird DW, Moheimani NR. The effect of gradual increase in salinity on the biomass productivity and biochemical composition of several marine, halotolerant, and halophilic microalgae. J Appl Phycol 2018;30:1453–64.
[175] Yeesang C, Cheirsilp B. Effect of nitrogen, salt, and iron content in the growth medium and light intensity on lipid production by microalgae isolated from freshwater sources in Thailand. Bioresour Technol 2011;102:3034–40.
[176] Rao AR, Dayananda C, Sarada R, Shamala T, Ravishankar G. Effect of salinity on growth of green alga Botryococcus braunii and its constituents. Bioresour Technol 2007;98:560–4.
[177] Amaro HM, Guedes AC, Malcata FX. Advances and perspectives in using microalgae to produce biodiesel. Appl Energy 2011;88:3402–10.
[178] Li Y, Horsman M, Wu N, Lan CQ, Dubois-Calero N. Biofuels from microalgae. Biotechnol Prog 2008;24:815–20.
[179] Fábregas J, Abalde J, Herrero C, Cabezas B, Veiga M. Growth of the marine microalga Tetraselmis suecica in batch cultures with different salinities and nutrient concentrations. Aquaculture 1984;42:207–15.
[180] Laing I, Utting SD. The influence of salinity on the production of two commercially important unicellular marine algae. Aquaculture 1980;21:79–86.
[181] Fon Sing S, Isdepsky A, Borowitzka M, Lewis D. Pilot-scale continuous recycling of growth medium for the mass culture of a halotolerant Tetraselmis sp. in raceway ponds under increasing salinity: a novel protocol for commercial microalgal biomass production. Bioresour Technol 2014;161:47–54.
[182] Arrigo KR, Sullivan CW. The influence of salinity and temperature covariation on the photophysiological characteristics of Antarctic sea ice microalgae. J Phycol 1992;28:746–56.
[183] Kirst G. Salinity tolerance of eukaryotic marine algae. Annu Rev Plant Biol 1990;41:21–53.
[184] Fogg G. Algal adaptation to stress—some general remarks. In: Rai LC, Gaur JP, editors. Algal adaptation to environmental stresses. Berlin: Springer; 2001. p. 1–19.
[185] Bartley ML, Boeing WJ, Corcoran AA, Holguin FO, Schaub T. Effects of salinity on growth and lipid accumulation of biofuel microalga Nannochloropsis salina and invading organisms. Biomass Bioenergy 2013;54:83–8.
[186] Sheehan J, Dunahay T, Benemann J, Roessler P. A look back at the U.S. Department of Energy's aquatic species program—biodiesel from algae. 1998.
[187] Wang ZT, Ullrich N, Joo S, Waffenschmidt S, Goodenough U. Algal lipid bodies: stress induction, purification, and biochemical characterization in wild-type and starchless Chlamydomonas reinhardtii. Eukaryot Cell 2009;8:1856–68.
[188] Richmond A, Boussiba S, Vonshak A, Kopel R. A new tubular reactor for mass production of microalgae outdoors. J Appl Phycol 1993;5:327–32.
[189] Rubio FC, Fernandez F, Perez J, Camacho FG, Grima EM. Prediction of dissolved oxygen and carbon dioxide concentration profiles in tubular photobioreactors for microalgal culture. Biotechnol Bioeng 1999;62:71–86.
[190] Tredici M, Materassi R. From open ponds to vertical alveolar panels: the Italian experience in the development of reactors for the mass cultivation of phototrophic microorganisms. J Appl Phycol 1992;4:221–31.
[191] Ugwu C, Aoyagi H, Uchiyama H. Influence of irradiance, dissolved oxygen concentration, and temperature on the growth of Chlorella sorokiniana. Photosynthetica 2007;45:309–11.
[192] Weissman JC, Goebel RP, Benemann JR. Photobioreactor design: mixing, carbon utilization, and oxygen accumulation. Biotechnol Bioeng 1988;31:336–44.
[193] Turner J, Todd M, Brittain E. The Inhibition of Photosynthesis by Oxygen I. Comparative physiology of the effect. Aust J Biol Sci 1956;9:494–510.
[194] Morhardt SS. Some effects of light intensity and oxygen concentration of Chlorella sorokiniana and an oxygen resistant strain. Houston, Texas: Rice University; 1968.
[195] Hartig P, Grobbelaar J, Soeder C, Groeneweg J. On the mass culture of microalgae: areal density as an important factor for achieving maximal productivity. Biomass 1988;15:211–21.
[196] Merrett MJ, Armitage TL. The effect of oxygen concentration on photosynthetic biomass production by algae. Planta 1982;155:95–6.
[197] Torzillo G, Bernardini P, Masojídek J. On-line monitoring of chlorophyll fluorescence to assess the extent of photoinhibition of photosynthesis induced by high oxygen concentration and low temperature and its effect of the productivity of outdoor cultures of Spirulina platensis (cyanobacteria). J Phycol 1998;34:504–10.
[198] Doucha J, Lívanský K. Productivity, CO_2/O_2 exchange and hydraulics in outdoor open high density microalgal (Chlorella sp.) photobioreactors operated in a Middle and Southern European climate. J Appl Phycol 2006;18:811–26.
[199] Miyachi S, Izawa S, Tamiya H. Effect of oxygen on the capacity of carbon dioxide-fixation by green algae. J Biochem 1955;42:221–44.
[200] Turner J, Brittain E. Oxygen as a factor in photosynthesis. Biol Rev 1962;37:130–70.
[201] Tredici MR. Photobiology of microalgae mass cultures: understanding the tools for the next green revolution. Biofuels 2010;1:143–62.
[202] Renaud SM, Thinh L-V, Lambrinidis G, Parry DL. Effect of temperature on growth, chemical composition and fatty acid composition of tropical Australian microalgae grown in batch cultures. Aquaculture 2002;211:195–214.
[203] Ras M, Steyer J-P, Bernard O. Temperature effect on microalgae: a crucial factor for outdoor production. Rev Environ Sci Bio/Technol 2013;12:153–64.
[204] Bordel S, Guieysse B, Muñoz R. Mechanistic model for the reclamation of industrial wastewaters using algal-bacterial photobioreactors. Environ Sci Technol 2009;43:3200–7.
[205] Lundholm N, Hansen PJ, Kotaki Y. Effect of pH on growth and domoic acid production by potentially toxic diatoms of the genera Pseudo-nitzschia and Nitzschia. Mar Ecol Prog Ser 2004;273:1–15.
[206] Sukenik A, Zmora O, Carmeli Y. Biochemical quality of marine unicellular algae with special emphasis on lipid composition. II. Nannochloropsis sp. Aquaculture 1993;117:313–26.
[207] Brown M, Garland C, Jeffrey S, Jameson I, Leroi J. The gross and amino acid compositions of batch and semi-continuous cultures of Isochrysis sp. (clone T. ISO), Pavlova lutheri and Nannochloropsis oculata. J Appl Phycol 1993;5:285–96.
[208] Abu-Rezq TS, Al-Musallam L, Al-Shimmari J, Dias P. Optimum production conditions for different high-quality marine algae. Hydrobiologia 1999;403:97–107.
[209] Fon-Sing S, Borowitzka M. Isolation and screening of euryhaline Tetraselmis spp. suitable for large-scale outdoor culture in hypersaline media for biofuels. J Appl Phycol 2016;28:1–14.
[210] Darvehei P, Bahri PA, Moheimani NR. A model for the effect of light on the growth of microalgae in outdoor condition. Comput Aided Chem Eng 2017:2737–42.
[211] Darvehei P, Bahri PA, Moheimani NR. Modeling the effect of temperature on microalgal growth under outdoor conditions. Comput Aided Chem Eng 2018:55–60.